Excavation Mechanics

Abstract

A mine structure is comprised of three basic building blocks, of which the starting block is an excavation. The development of two separate adjacent excavations results in the formation of the second kind of building block, namely a pillar. The formation of many excavations and pillars requires consideration of a third type of building block, being the surrounding strata. This chapter presents the basic principles of how the rock mass responds to the formation of single and multiple excavations in the same mining horizon.

The changes that take place in the rock mass in the immediate vicinity of an excavation are conceptualised using a number of simple two-dimensional models. The width of an excavation is progressively increased in order to induce caving of the immediate roof strata that, with further increases in excavation span, ultimately result in subsidence of the surface over and outside of the footprint of the excavation. The basic physical and mechanical principles established in Chap. 2 are applied and further developed to account for how mining span, mining depth and the structural and mechanical properties of the superincumbent strata affect the stability of this strata and the maintenance of ground control in the vicinity of active mining faces.

These principles provide the basis for considering three situations where risk may be elevated when employing high percentage extraction mining methods. The situations relate to mining under strong massive strata; to mining in environments subjected to elevated horizontal stress; and to mining at shallow depth. Theoretical and practical aspects associated with each circumstance are discussed. This provides insight into the type of controls required to effectively manage risk.

3.1   Introduction

A mine structure is comprised of three basic building blocks, of which the starting block is an excavation. The development of two separate adjacent excavations results in the formation of the second kind of building block, namely a pillar. The formation of many excavations and pillars requires consideration to be given to the third type of building block, being the surrounding strata. This chapter presents the basic principles of how the rock mass responds to the formation of an excavation. Coal pillar systems are discussed in a similar manner in Chap. 4, followed by interaction between workings in the same seam and in adjacent seams in Chap. 5. The behaviour of the superincumbent strata is discussed specifically in Chap. 10 but also in some detail in most chapters. This reflects the interdependence between the three fundamental elements, which does not permit each to be discussed in complete isolation.

3.2   Excavation Response

The changes that take place when an excavation is developed in a rock mass can be conceptualised using a number of simple two-dimensional models that assume the rock mass is free of defects, behaves elastically and is outside the zone of influence of other excavations. Figure 3.1a shows how the outside surfaces of an isolated portion of this rock mass are loaded by primitive (or virgin) stresses, with the rock inside the boundary of a proposed excavation providing the required internal support to maintain the whole system in a state of equilibrium. When the supporting rock is removed to form the excavation, the stresses on the outer surfaces of the rock mass remain unchanged, but the perimeter of the newly created excavation becomes stress free as shown in Fig. 3.1b. Hence, the initial equilibrium is destroyed and the system of forces must be rearranged to restore equilibrium.

To create the new stress free boundary, stresses must be induced which are equal in magnitude but
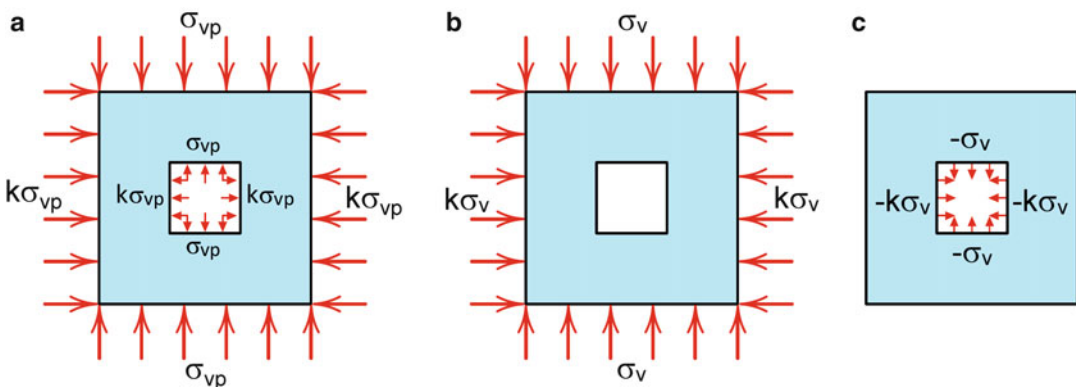

Fig. 3.1 Primitive (**a**), resultant (**b**) and induced (**c**) stresses around an underground excavation (Adapted from Salamon and Oravecz 1976)
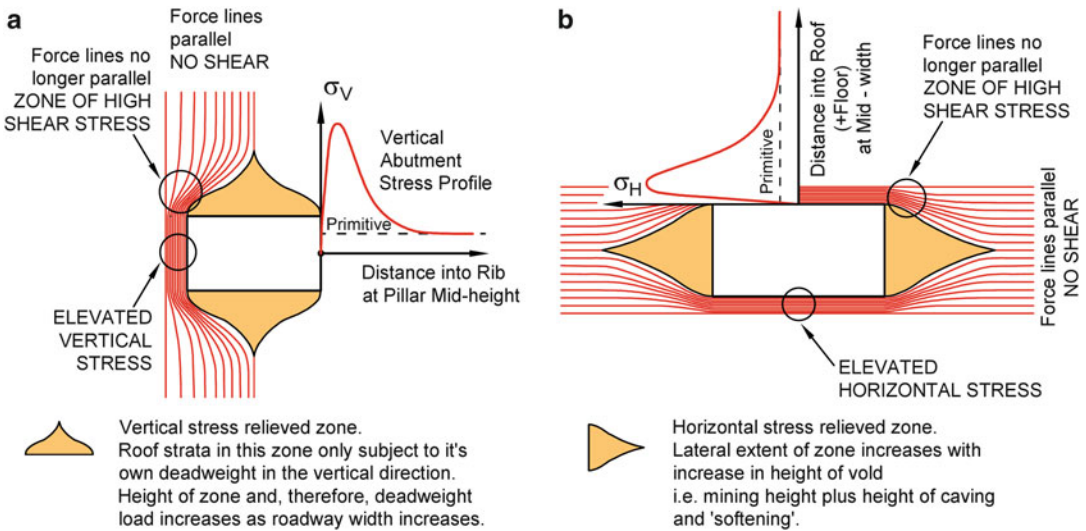
Fig. 3.2 Stress trajectories around an excavation

opposite in direction to the compressive primitive stresses that were acting on the excavation boundaries prior to mining. As a result of these induced tensile stresses, shown in Fig. 3.1c, the sides, roof and floor of the excavation can be visualised as being pulled inwards. Because of the upward pull on the floor and the downward pull on the roof, a high vertical stress can be expected in the sidewalls of the excavation.

Plotting of stress trajectories (or streamlines) as shown in Fig. 3.2 provides another means for visualising these responses. The figure shows how an excavation acts as an obstruction to stress flow, with the vertical and horizontal stresses that used to pass through the unexcavated rock mass in parallel trajectories having to deviate around the new excavation. In the case of vertical stress (Fig. 3.2a), this results in:

- increased vertical stress in the sidewalls of the excavation;
- the generation of shear stresses which are a maximum in the vicinity of the excavation corners; and
- a wedge or dome of material in the immediate roof and the immediate floor that, other than for self weight, is relieved of vertical stress.

Analogous conclusions can be drawn with regard to horizontal stress (Fig. 3.2b). It can be concluded from combining these stress trajectory models that:

- increasing excavation width increases vertical compressive stresses in the sidewalls of the excavation; and
- increasing excavation height increases horizontal compressive stresses in the roof and floor strata of the excavation.

In summary, the induced vertical stresses in the immediate roof of an excavation are independent of the size and shape of the excavation and are only a function of depth of mining. The induced horizontal stresses are a function of the shape and size of the excavation, the depth of mining, and the nature and behaviour of the immediate roof, the upper roof and the coal seam. Similar considerations apply in regard to the floor horizon.

Displacement of the rock mass surrounding an excavation is determined by the induced stresses, while rock mass failure is determined by the resultant stresses. Up to the onset of yield in the rock mass, excavation **closure,** or **convergence,** is due solely to elastic rebound. Although horizontal compressive stresses are induced in the roof and floor strata of an excavation, the resultant horizontal stresses may still be tensile, depending on depth, excavation geometry and primitive horizontal to vertical stress ratio.
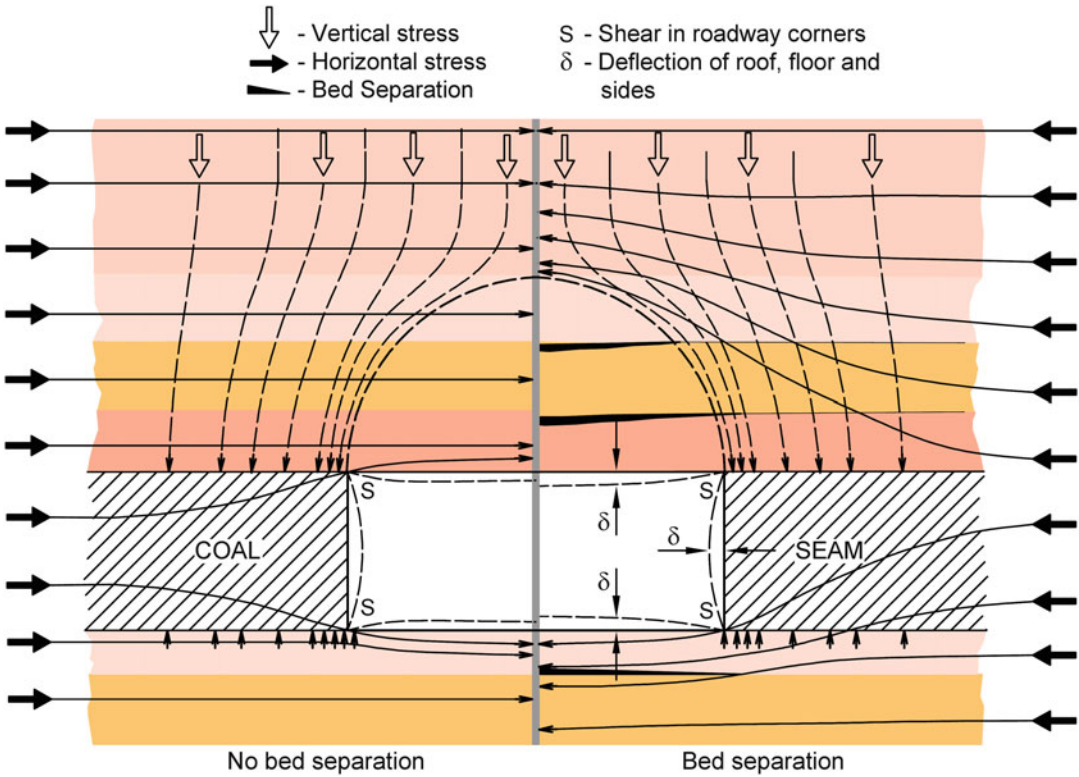
Fig. 3.3 Redistribution of stress around a narrow excavation, before and after delamination of immediate roof and floor strata (Partially adapted from Menzies c1970)

Figure 3.3 shows in more detail the manner in which stresses and strains are distributed around an excavation prior to the onset of caving of the immediate roof. The vertical stress distribution gives rise to the formation of a dome shaped zone, referred to as a **pressure arch**, with the weight of the strata outside of the pressure arch being transferred to the abutments of the excavation. The strata within the pressure arch effectively constitute a decoupled immediate roof for the excavation, being vertically destressed and loaded transversely by only its own weight and axially by lateral forces.

In coal mines, the immediate roof and floor strata are usually bedded due to the sedimentary origin of coal deposits. Bedding planes are characterised by low to zero tensile strength normal to the bedding planes and low shear strength relative to that of intact rock. Hence, bedding planes constitute potential slippage planes and can effectively divide the roof strata into an

assembly of thin rock beams, thereby permitting the immediate roof to sag under its own weight. The sense of slip causes inward displacement towards the centreline of the span and decreases with height into the roof, so that there is a tendency for the beds to delaminate, or decouple, in both the immediate roof and the immediate floor. In the case of the immediate roof strata, bed separation results in a loss of load sharing with upper beds and the transfer of horizontal stress to higher horizons in the roof as shown on the right hand half of Fig. 3.3. Stress transfer to deeper horizons in the floor is not so prevalent but does occur with the onset of floor heave.

Bedded strata can be conceptualised as a series of plates. If an excavation is long compared to its width, roof strata remote from the ends of the excavation can be visualised as behaving as beams when subjected to transverse load and as columns when subjected to axial load. Hence, classical beam theory and linear

arch theory find application for analysing the behaviour of the immediate roof of an excavation, albeit that limitations are associated with these approaches (see Sect. 2.7 and Chap. 7).

It is important to appreciate that ground failure is not induced by just an increase or decrease in one component of stress but rather by a change in deviator stress (see Sect. 2.6.2). The biggest change in deviator stress results from the total removal of confinement, which causes a triaxial state of stress to revert to a uniaxial state of stress. The formation of an excavation results in the rock mass surrounding the excavation undergoing this transition. Hence, whilst failure is often attributed to high abutment stress, reduction in confinement is more likely to be the primary cause.

3.3   Caving Mechanics

3.3.1   Basic Principles

It is convenient to introduce the basic principles of caving mechanics and goaf reconsolidation by considering the simple case of a single (isolated) total extraction panel of width, W, assumed to be at low to moderate depth, H, say less than 200 m. Although the principles under consideration are relevant to mining at greater depth, they can rarely be extrapolated directly as a design tool to deeper situations because they fail to adequately reflect the mechanics of the loading system, in particular, the stiffness of the superincumbent strata.

The minimum plan dimension, or lateral dimension, of an excavation is the critical dimension that controls the response of the rock mass. In underground coal mining, deliberate caving of an excavation is usually undertaken only as mining retreats from a panel. This means that the length of the excavation is the critical dimension up until the point where the excavation takes on a square shape. Thereafter, the excavation width becomes the critical dimension. The minimum excavation dimension at any point in time is referred to as the **span**.

Ultimately, with increasing excavation span, the immediate roof loses its capacity to bridge across the excavation and begins to cave. If failure is associated with shear at the abutments then near vertical failure surfaces may extend for several metres up into the roof. Otherwise, as illustrated in Fig. 3.4, the immediate roof caves out over the excavation. Because caved rock strata consist of blocks of rock which rotate when they fall, the caved rock material occupies a greater volume than when in situ. This behaviour is known as **bulking**. Weak laminated strata, such as shales and mudstones, generally cave at a steeper angle and bulk less than stronger and more massive strata, such as sandstone. With increasing excavation span, the point is reached where due to the combined effects of caving, bulking, lowering of the roof and uplift of the floor, the caved material comes into contact with

Fig. 3.4 An example of how the immediate roof strata cantilevers out over the goaf
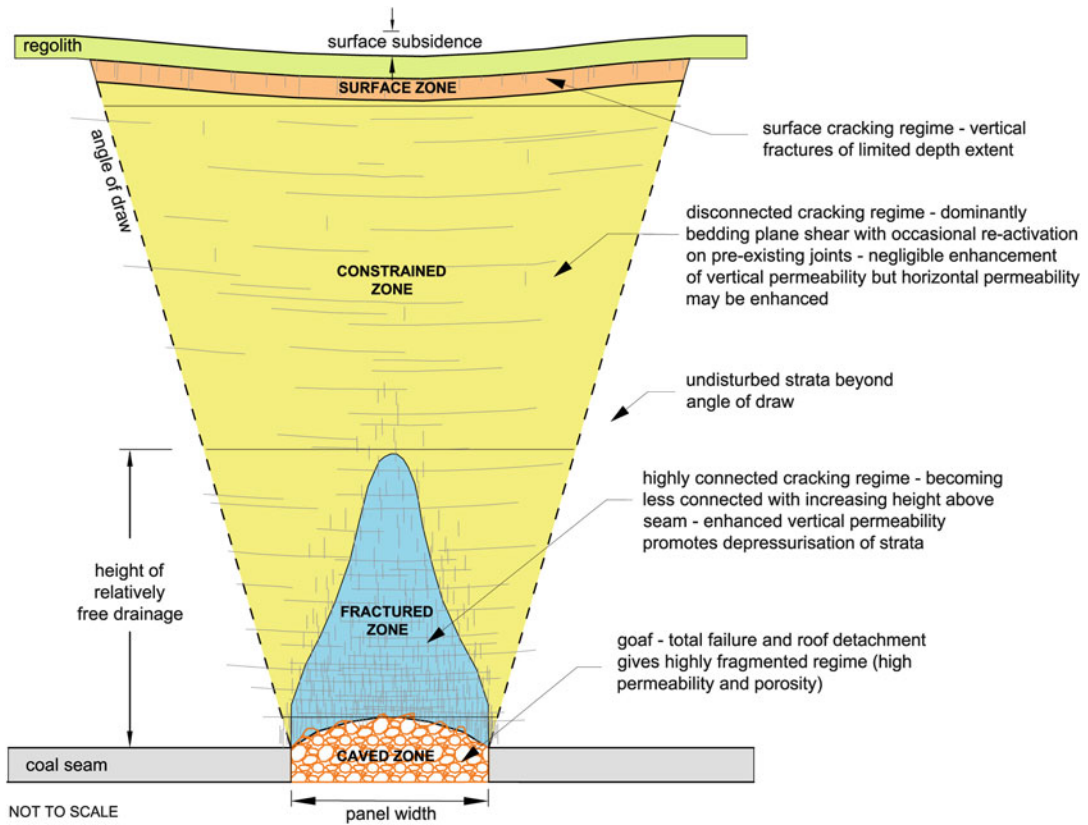
Fig. 3.5 A conceptual four zone model of caving and fracturing above an excavation (Courtesy of Dr Colin Mackie)

the strata above and provides support to it. This defines the **caving height** and the limit of the **caved zone**, shown in Fig. 3.5.

The overlying strata continue to sag as excavation span increases but the support and cushioning provided to this strata by the caved material prevents them from unravelling and increasing appreciably in volume. Nevertheless, considerable fracturing and bedding plane shear stills occurs within the sagging strata, resulting in a well developed and connected vertical and horizontal fracture network that becomes less extensive and connected with distance above the excavation. This network defines the **fractured zone** (Fig. 3.5).

The lateral extent of roof strata sag increases with distance above the excavation, resulting in a decreasing rate of deflection, or curvature, in the upper roof strata and a corresponding reduction in shear and bending stress. This zone is referred to as the **dilated zone** in some models.

Given sufficient depth, a point is reached where the tensile stresses become too low in the upper strata to cause joints to open or new vertical fractures to develop on a regular or continuous basis. Horizontal fracture planes are still likely to be activated due to sagging strata sliding past each other but the magnitude of these displacements also reduces as curvature decreases. The zone in which this behaviour occurs is referred to as the **constrained zone** (Fig. 3.5), and is characterised by strata that have not suffered a significant alteration of their physical properties. Stress measurements, field observations of subsidence behaviour and numerical modelling show that the constrained zone can sustain elevated levels of horizontal stress.

Strata response close to the surface is influenced by the surface being in an unconfined state. In flat topography, this response essentially mirrors that of a beam (or plate). Within this
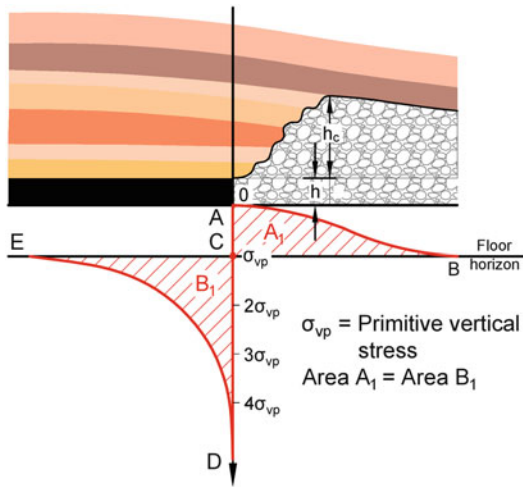
Fig. 3.6 Stress distribution at floor horizon around a caved excavation

so-called **surface zone** (Fig. 3.5), ground behaviour is characterised by bedding plane shear and tensile and compressive cracking of limited vertical extent.

Figures 3.5 and 3.6 show these various zones to be bounded by a conceptual **angle of draw.** The angle of draw defines the limit of the vertical component of surface displacement and, hence, the extent of the subsidence trough. It is the angle between two lines drawn from the edge of the mine workings, one a vertical line and the other a line to the limit of **vertical displacement, V_z,** on the surface. Although the concept of a line demarcating the boundary between moving and stationary ground is theoretically untenable, nevertheless the approach finds extensive application and is helpful in conceptualising ground behaviour. Angle of draw is discussed further in Chap. 10.

There is no one universally accepted model of subsurface behaviour. While all models are based on similar principles, there is considerable variation in terminology, the number of zones, and the proposed thickness of each zone. This is usually a reflection of the site specific lithology and the nature of the subsidence impact being assessed. Subsurface subsidence behaviour models are discussed further in Sect. 10.3.

Once the caved material comes into contact with the overlying strata, further increases in

excavation span cause progressive compaction of the caved material, thereby increasing its stiffness and the level of support it provides to the superincumbent strata. If the excavation span is sufficiently wide and the depth of mining not too great, the stiffness of the superincumbent strata will be reduced to zero, resulting in the full weight of the overburden being carried by the caved material and transferred through to the floor at some distance back into the goaf, as shown in Fig. 3.6. Vertical displacement of the surface reaches a maximum value above this point.

The panel span-to-depth ratio, W/H, at which the stiffness of the overburden is reduced to zero corresponds with the vertical surface displacement above an isolated panel reaching its maximum possible value and is referred to as the **critical** width-to-depth ratio, W_c/H. Larger panel width-to-depth ratios are referred to as being **supercritical** and smaller panel width-to-depth ratios as being **subcritical**. It is very common in subsidence engineering to normalise vertical displacement, V_z, by dividing it by mining height, h, and then plotting this ratio (V_z/h) against W/H. This is an example of the care that must be taken when working with normalised, or dimensionless, relationships since mining height has minimal influence on subsidence at subcritical panel width-to-depth ratios.

That portion of the weight of undermined strata not carried by the floor of an excavation at a given W/H ratio is transferred onto the abutments of the excavation, giving rise to abutment stress. Hence, in the two-dimensional representation shown in Fig. 3.6, the area of the destressed zone 'ABC' has to equal the area of the elevated stress zone 'CDE'. The actual shape and size of these zones depends on many factors, including the caving and compaction characteristics of the immediate roof, the stiffness of the overburden, the excavation width-to-depth ratio and the extraction height. If the rock mass is considered to be elastic and homogeneous then, in theory, the tangential stress at the right angled corner of a rectangular opening approaches infinity. This can be managed by profiling the corners of the excavation. In practice, the corners of rectangular excavations yield, causing the peak abutment stress front to migrate

into the solid. Guttering can be an expression of this yielding process.

Weak strata, such as shales and mudstones, cave at a steeper angle than stronger strata such as sandstones and conglomerates. Typically, the overall caving angle, β, (measured from the mining horizon) is observed from the goaf edge to be in the range of 65°–80° for weak strata and 55°–65° for stronger strata. Some massive strata may cantilever a considerable distance out into the goaf before breaking and relieving abutment stress. This cyclic process of caving, convergence and recompaction is commonly referred to as **periodic weighting**.

Bulking and compaction characteristics determine the rate that the goaf generates support to the undermined strata, and the distance back into the goaf to restoration of full overburden support. Caving and subsidence progress relatively uniformly through bedded and weak strata, while more massive and strong strata often subside in a discontinuous manner as a series of discrete blocks that separate at distinct horizons within the superincumbent strata (see for example, Hardman 1971; Galvin et al. 1982; Mills and O'Grady 1998). The **bulking factor, k**, is defined as the ratio of the total volume of the caved material to its solid volume. For situations where caving progresses uniformly up into the roof strata, **the initial bulking factor, k_i,** is given by Eq. 3.1.

$$k_i = \frac{h + h_c}{h_c} \qquad (3.1)$$

where

$h = $ *mining height*
$h_c = $ *maximum initial height of caving above mining roof*

hence

$$h_c = \frac{h}{k_i - 1} \qquad (3.2)$$

Equation 3.2 shows that mining height has a significant influence on the height of caving. A steep caving angle and a low initial bulking factor, k_i, of the order of 1.1–1.3, are usually associated with highly laminated strata because they tend to fall like a deck of cards, with minimal rotation and relative displacement of blocks, as illustrated in Fig. 3.7. Caving angles are flatter and block rotation occurs to a much greater extent in stronger and more massive strata, as illustrated in Fig. 3.8, with initial bulking factors for sandstone, for example, being in the range of 1.4–1.5 (Galvin et al. 1982). Although in reality caving may be interrupted by strong or massive beds, the concept of bulking factor still provides a foundation for understanding goaf behaviour and reconsolidation and the loading of support systems in total extraction mining.

The load-deformation relationship for goaf material is not linear, with compaction causing a reduction in bulking factor and an increase in stiffness. The hostile nature of a goaf environment presents major challenges to measuring consolidation and strain hardening

Fig. 3.7 A fall of ground at an intersection, illustrating attributes of a steep caving angle and a low initial bulking factor associated with weak laminated strata

Lip of fall

Fallen material

21 AUG 2008

Fig. 3.8 Caving of a moderately strong massive roof, illustrating attributes of a flat caving angle and a high initial bulking factor
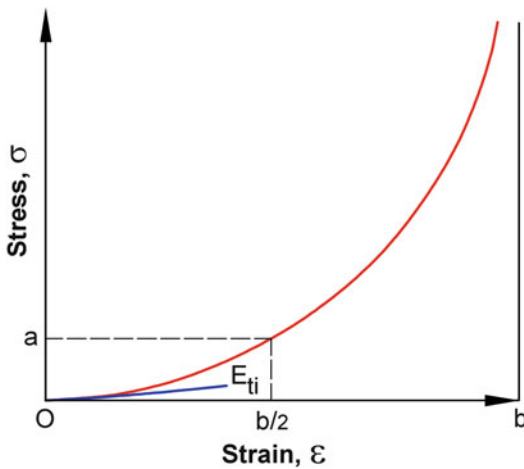

Fig. 3.9 Stress-strain characterisation of goaf backfill (After Ryder and Wagner 1978)

characteristics in the field, with attempts by Jacobi (1956), Wade and Conroy (1980), Haramy and Fejes (1992), Campoli et al. (1990), Wang and Peng (1996) and Kelly et al. (1998) and others producing variable outcomes.

In the absence of experimental work on the physical properties of goaf material, Salamon (1966) explained goaf consolidation and surface subsidence behaviour by adopting a soil mechanics relationship between porosity and pressure given by Kezdi (1952). The behaviour of backfill in goaf areas also provides insight into goaf consolidation behaviour. Ryder and Wagner (1978) described the consolidation behaviour of goaf backfill by the stress-strain relationship shown in Fig. 3.9 and concluded that Eqs. 3.3 and 3.4 describe this relationship surprisingly well.

$$\sigma_f = \frac{a\varepsilon}{b - \varepsilon} \tag{3.3}$$

where

$\sigma_f = $ *fill reaction stress*
$b = $ *maximum compaction of backfill material*
$a = $ *fill reaction stress at a strain value of* 0.5*b*

Equation 3.3 can be reduced to:

$$\sigma_f = \frac{E_{ti}\varepsilon}{\left(1 - \dfrac{\varepsilon}{\varepsilon_m}\right)} \tag{3.4}$$

where

$\sigma_f = $ *fill reaction stress*
$E_{ti} = $ *initial tangent modulus for the stress–strain curve of the fill material*
$\varepsilon = $ *compaction strain at any point in time*
$\varepsilon_m = $ *the maximum possible strain that can be developed in the fill*
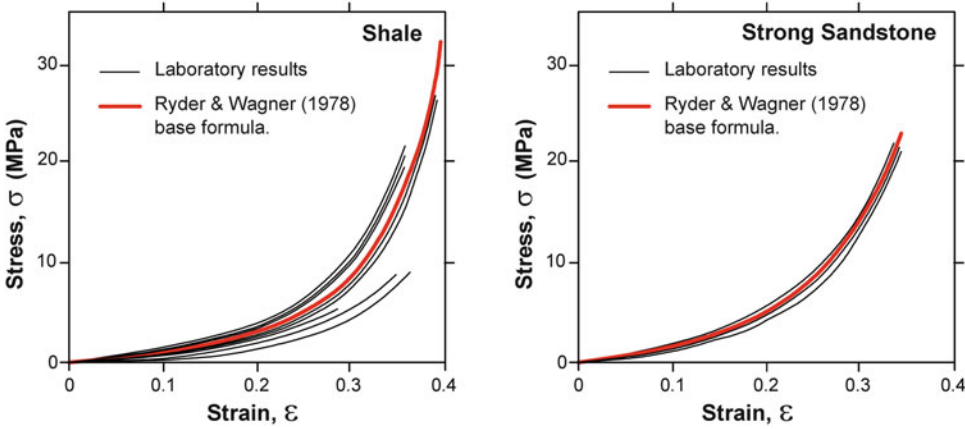
Fig. 3.10 Comparison between analytically and laboratory derived stress-strain relationships for two types of goaf material (Adapted from Pappas and Mark 1993)

Salamon (1990) showed that there was a reasonable body of evidence, including that of Ryder and Wagner (1978), to suggest that Eq. 3.5 borrowed from studies of granular material may be a credible descriptor of the relationship between bulking factor and overburden pressure:

$$k = \frac{p + k_i p_c}{p + p_c} \qquad (3.5)$$

where

k_i = initial bulking factor
k = bulking factor at any point in time
p = applied overburden stress
p_c = a material constant ranging from 0.5 MPa to 5.0 MPa for coal measure rocks

Rearranging Eq. 3.5 produces the expression given by Eq. 3.6 for applied overburden stress:

$$p = \frac{p_c (k_i - k)}{k - 1} \qquad (3.6)$$

Salamon noted that Eq. 3.4 could be equated with Eq. 3.6, thus enabling the material constant, p_c, to be defined by Eq. 3.7.

$$p_c = E_{ti} \varepsilon_m \qquad (3.7)$$

Pappas and Mark (1993) reported that numerical modellers have used estimates of goaf modulus that range from around 7 MPa (~1000 psi) to over 2.1 GPa (~300,000 psi), with such wide variations greatly affecting the outcomes of the numerical analyses. Based on laboratory scaled tests, the authors developed the formulae given by Eqs. 3.8 and 3.9 for secant and tangent modulus of goaf material (note that these formulae cannot be converted to metric equivalents by simply expressing stress in metric units). They concluded that although these formulae could not be assumed to describe the moduli of all goaf material types, they produced outcomes that corresponded reasonably well with theoretical solution curves developed by Ryder and Wagner (1978) and Salamon (1990). Two examples of this correlation are shown in Fig. 3.10.

$$E_s = 2.36\sigma + 1360 \qquad (3.8)$$

$$E_t = 0.00181\sigma^2 + 9.33\sigma + 294 \qquad (3.9)$$

where

E_s = Secant modulus (psi)
E_t = Tangent modulus (psi)
σ = Stress level due to overburden (psi)

The magnitude and distribution of floor pressure beneath the goaf is also a function of the stiffness of the upper roof strata, since it is the displacement of this strata that provides the driving force for compaction. The displacement is determined by the elastic modulus, span and
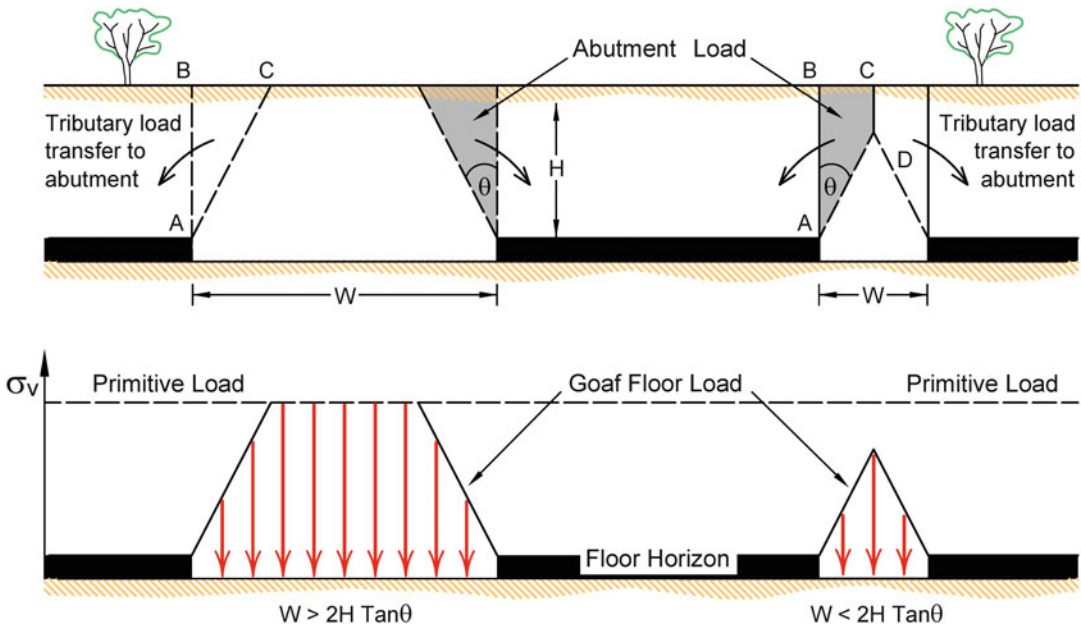
Fig. 3.11 Simplified model of load transfer around an isolated excavation (Adapted from Salamon 1991a, after King and Whittaker 1971)

thickness of the individual overlying stratum and how they behave as a composite. Quantifying the manner in which the relative stiffnesses of the goaf material, the overlying undermined strata and the surrounding strata determine the load distribution around an excavation is complex and requires the use of numerical modelling.

Nevertheless, a simplified two-dimensional model proposed by King and Whittaker (1971) provides a basis for conceptualising how abutment load is generated around an isolated panel, although as suspected by Mark and Bieniawski (1987), this model is not as straightforward as implied by its developers. The model assumes the superincumbent strata shears off over the goaf at some **shear angle**, θ, measured from the vertical, as shown in Fig. 3.11. It forms the basis of a number of others in which the term 'shear angle' is referred to variously as the **abutment angle**, ɸ, measured from the vertical, and the **angle of caving**, β, and the **angle of break**, β, where β is measured from the horizontal. The abutment angle concept equates abutment load to the equivalent weight of a wedge of rock projecting off the abutment at an angle, ɸ. The

weight of this rock is apportioned to the sides of an excavation in accordance with tributary area theory, which distributes overburden load to a pillar or abutment on the basis of its area of influence as defined by the loci of mid-points to adjacent pillars and abutments (see Fig. 3.11 and also Sect. 4.3.2).

Figures 3.12 and 3.13 show examples of the concept of shear angle in practice above longwall panels at shallow depth in weak immediate roof strata. In the case of Fig. 3.13, overall shear angle ranged from 18.5° to 23°.

According to these models, once the shear angle daylights at the surface, any further increase in span results in full overburden load being transmitted through the goaf to the floor of the excavation. Therefore, the daylight span should correspond to the critical span at which full surface subsidence, or vertical surface displacement, develops (ignoring additional time-dependent compaction and settlement, which typically makes up about 10 % of the final vertical displacement).

There are a number of limitations associated with applying the concept of shear angle to

Fig. 3.12 Exposed goaf showing angle of break at the side abutment of a shallow, supercritical width, longwall panel in a weak immediate roof strata environment at a depth of approximately 70 m
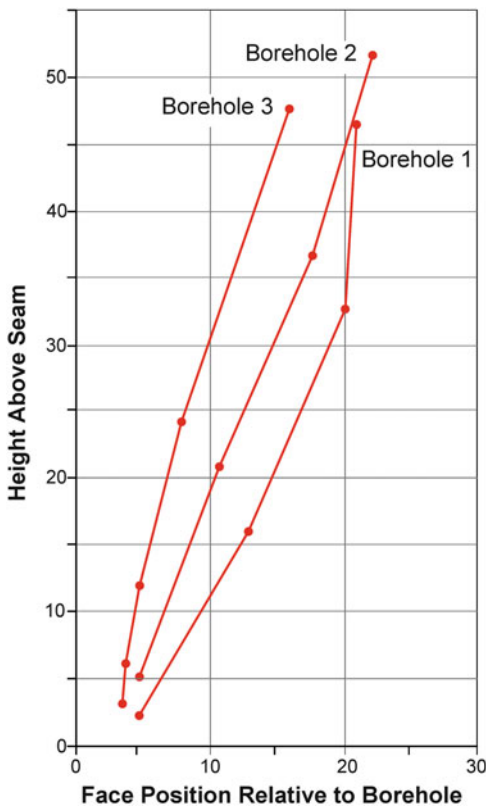

Fig. 3.13 Caving behaviour in weak shale roof above a longwall panel at a depth of mining of 115 m as determined from borehole extensometers (After Galvin et al. 1982)

calculate abutment load and these can affect the reliability of design outcomes. The limitations include that the model is insensitive to differences in the caving behaviour of individual strata (which can be extreme); it has no regard to **discontinuous subsidence**, whereby subsidence is impeded by competent strata forming a bridge somewhere within the superincumbent strata; it may not adequately approximate the shape of a pressure arch; and it has no regard to the stiffness of the superincumbent strata. The potential for these limitations to arise is reflected in the range in shear angles for individual strata of $16°–29°$ measured (from the vertical) in South Africa using borehole extensometers (Galvin et al. 1982), and $5°–35°$ reported by Peng (2008) on the basis of reviewing literature. Internationally, a range of surface subsidence data, such as that shown in Fig. 3.14, indicate that a panel width-to-depth ratio of at least 1 is required to induce full subsidence over an isolated coal mine excavation. This corresponds to an overall shear angle of $26.5°$.

The most significant limitation associated with equating abutment load to an overall shear angle, or so-called abutment angle, is that the concept has no regard to the stiffness of the
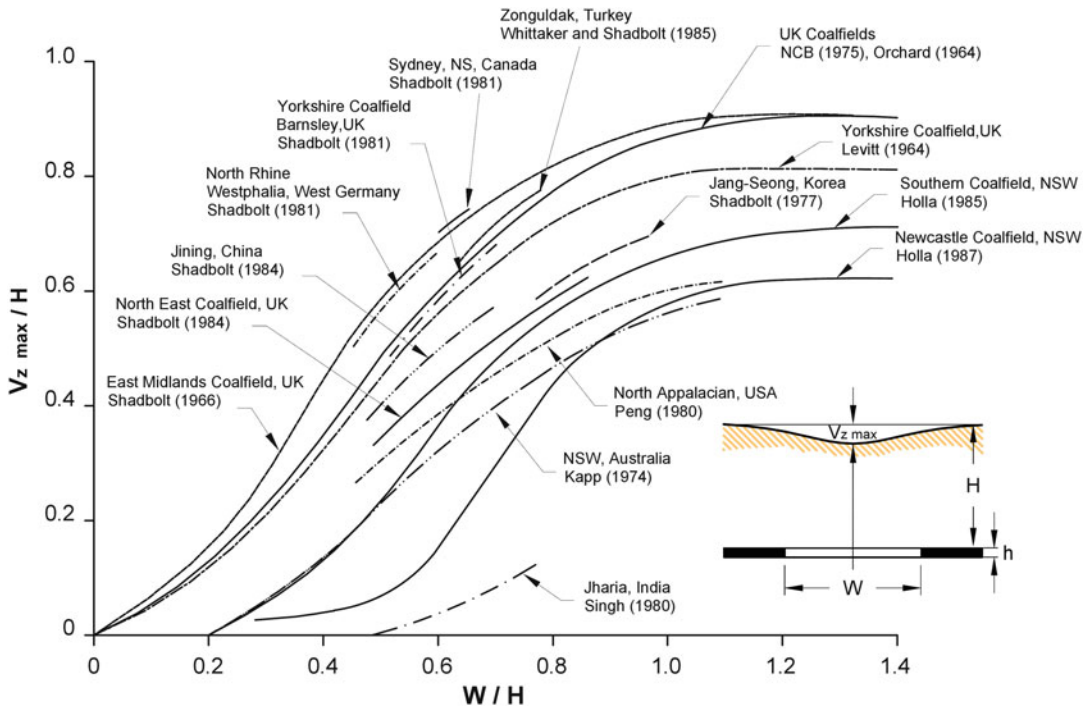
Fig. 3.14 Influence of extraction panel width-to-depth ratio on maximum vertical surface displacement, $V_{z\,max}$, expressed as a fraction of mining height, for isolated total extraction panels (Adapted from Whittaker and Reddish 1989, page 355, copyright Elsevier 1989)

superincumbent strata, although there have been attempts to take this into account by using different angles for different mining districts. Profiles of vertical displacement at the surface (often generically referred to as 'surface subsidence') are a reflection of the stiffness of the superincumbent strata and, therefore, give valuable insight into the distribution of superincumbent strata load. This is illustrated by the vertical surface displacement profiles shown in Figs. 3.15 and 3.16, which are associated with two sets of 210 m wide longwall panels under not very dissimilar geological conditions, one at a depth of ~80 m and the other at a depth of ~500 m.

When the depth of cover is low (typically less than 150 m) and the total excavation width-to-depth ratio, W/H, for an individual panel is high (typically, at least one and often higher), the stiffness of the superincumbent strata over a shallow excavation can reduce to zero as it is being extracted, resulting in vertical surface displacement over that panel developing virtually

independently of that over adjacent panels. The abutment load on the interpanel pillars is relatively low because the depth of cover is shallow and because the superincumbent strata over the flanking excavations does not dome and form a bridge. This results in near symmetrical profiles of vertical surface displacement, such as those shown in Fig. 3.15, as soon as each panel is extracted. In these circumstances, compression of the interpanel pillars (chain pillars) and their immediate roof and floor strata makes only a minor contribution to vertical displacement and over 90 % of the final vertical displacement at a surface point is usually reached within weeks of it being undermined. The measured vertical surface displacement above interpanel pillars in these circumstances may largely reflect interaction of neighbouring subsidence troughs, illustrated in Fig. 3.17, rather than compression of the pillar system and surrounding strata.

The situation is quite different at depth. Figure 3.16 shows that limited vertical surface
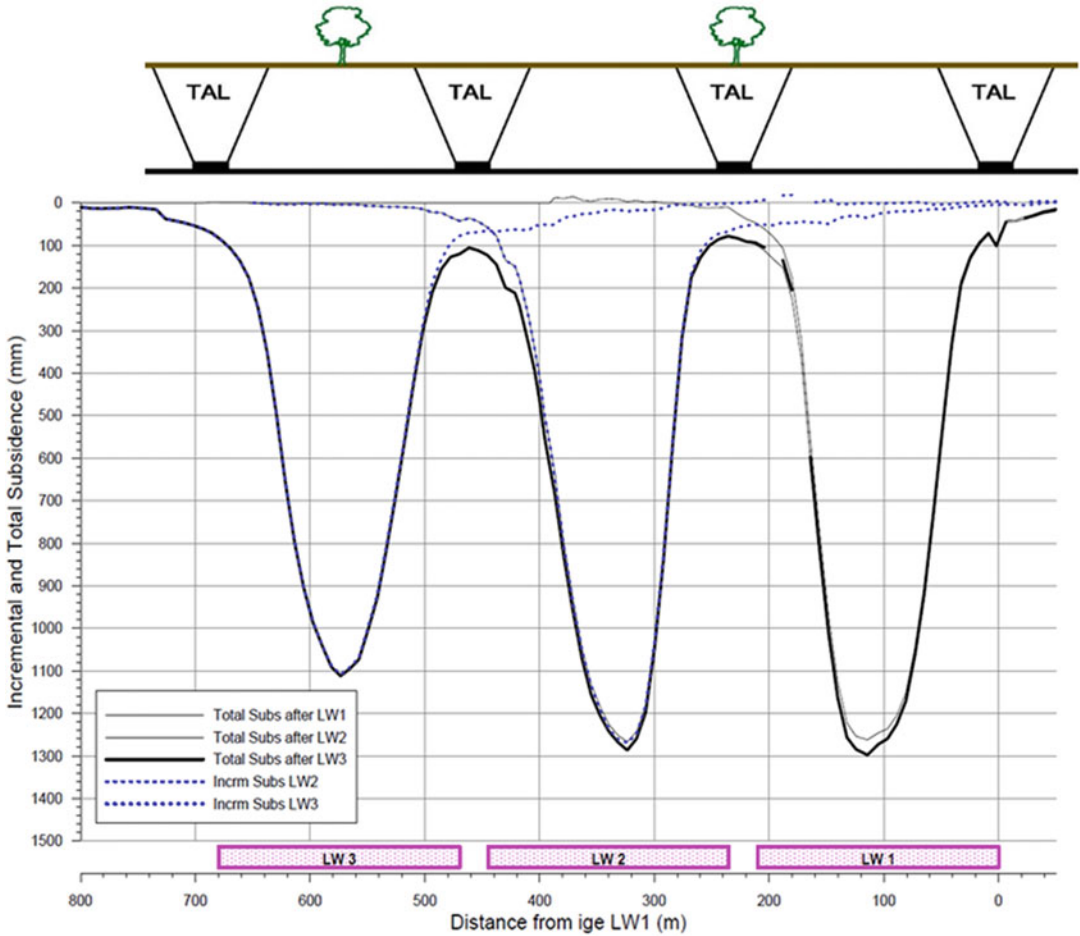
Fig. 3.15 Vertical surface displacement profiles over 210 m wide longwall panels at a depth of around 80 m (W/H = 2.6) showing how maximum surface displacement develops virtually independently of subsequent panel extraction at shallow depth, consistent with tributary area load (TAL) based on the concept of an abutment angle

displacement occurred over the first longwall panel, being LW 401, when it was extracted. Extraction of LW 402 resulted in a large step increase in vertical displacement over LW 401. This additional displacement is referred to loosely as **incremental subsidence**. The overall vertical surface displacement profile is found by summing the incremental subsidence profiles. The pattern of change in the incremental subsidence profiles as more longwall panels are extracted is evidence of a progressive reduction in the stiffness of the superincumbent strata, resulting in increased compression of the pillar system and surrounding roof and floor strata.

Vertical surface displacement over LW 401 continued to increase in increments during extraction of at least the next four longwall panels, albeit at a diminishing rate. Once the stiffness of the overburden had been reduced to zero, incremental vertical displacement reached a steady state.

The behaviours shown in Figs. 3.15 and 3.16 are similar to those associated with Longwall 103 at Gordonstone Colliery and Longwall 28 at Appin Colliery, which were the sites of microseismic research reported by Hatherly et al.(1995), Kelly et al.(1998) and Kelly and Gale (1999). Figure 3.18 shows the profile of
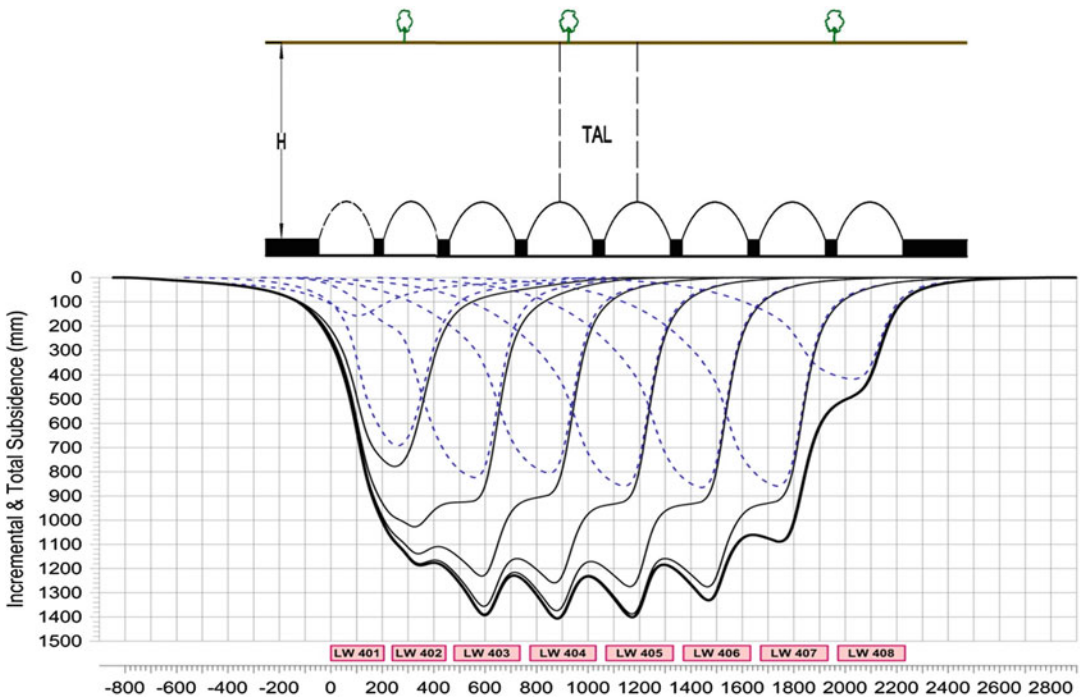
Fig. 3.16 Vertical surface displacement profiles over 210 m wide longwall panels at a depth of around 500 m (W/H = 0.42) showing how maximum vertical surface displacement develops incrementally at depth as subsequent panels are extracted and not in accordance with tributary area load (TAL) based on the concept of abutment angle
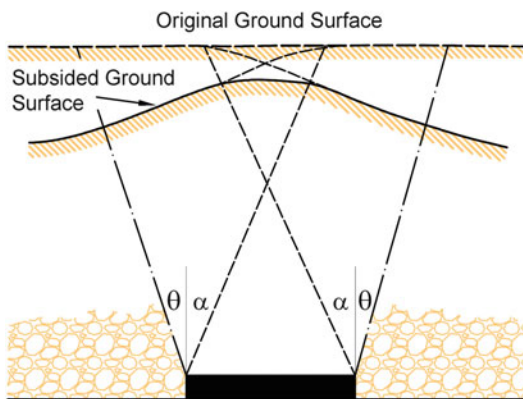

Fig. 3.17 Illustration of how overlap in subsidence profiles results in vertical displacement over an interpanel pillar

vertical surface displacement and microseismic activity plots associated with extracting a 3 m thick seam at a depth of around 235 m utilising a 250 m wide longwall at Gordonstone Colliery. Kelly et al. (1996) and Hatherly and Luo (1999)

report that Longwall 103 was a benign setting where the geology above and below the seam had relatively uniform properties, there were no geological structures, and the horizontal stress field was not severely distorted by previous mining panels. Thus, the researchers considered that they were able to observe what might be called 'classical' behaviour. The immediate roof and floor were particularly weak, with UCS values of only 5–15 MPa, while some bands in the upper roof strata had UCS values of about 50 MPa (Kelly et al. 1998). Of particular note is that the upper 70 m of overburden comprised unconsolidated material. This could be anticipated to both function as a surcharge load and to increase the effective panel width-to-depth ratio (due to the reduced thickness of solid rock cover).

The microseismic events were located to an accuracy of about 5 m and, as shown in Fig. 3.18b, d, confined mainly to within 120 m above the mining horizon and 50 m below it. The events were located within an envelope rising

above the gateroads at an angle of about 16° to the vertical and sweeping ahead of the face on an arcuate shape (Fig. 3.18c). At seam level in the centre of the panel, the envelope was some 70 m ahead of the face and rose at an angle of about 50° to the vertical over the face (Fig. 3.18d). Pore pressures began to increase markedly at around 200 m ahead of the face, at distances coinciding with the onset of the microseismic activity. Kelly and Gale (1999) suggested that such rises in pore pressure contribute to the rock mass fracturing at such long distances ahead of the longwall face.

The pattern of seismicity was remarkably symmetric, with events located equally on the tailgate and maingate sides of the panel. Microseismic activity did not necessarily coincide with any marked deterioration in ground conditions in mine roadways or on the longwall face and there was no suggestion of a cyclic pattern of failure. The microseismic events were attributed to shear failure, with failure planes parallel to and rising over the longwall face. Bedding plane shear, if it was occurring, did not cause seismic activity sufficient for it to be observed. These microseismic monitoring outcomes, supported by profiles of vertical surface subsidence, are consistent with the residual stiffness of the superincumbent strata being reduced to a negligible value over each individual longwall panel as soon as it was undermined, so that the panels largely acted independently of each other. In circumstances such as these where mining is taking place at relatively shallow depth beneath strata that
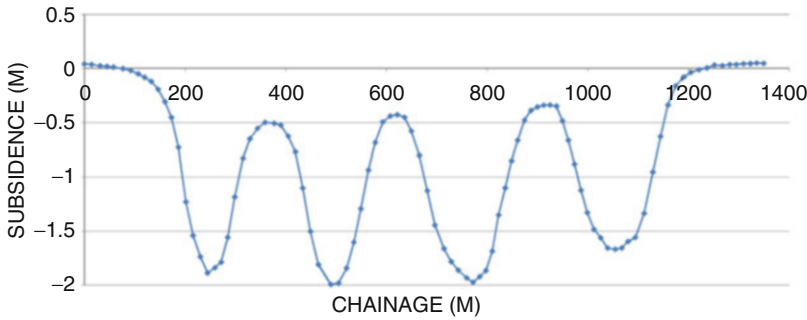
Fig. 3.18 Surface subsidence profile and microseismic event location plots associated with extracting Longwall 103 at Gordonstone Colliery. (**a**) Transverse vertical surface displacement profile (H = 235 m, $H_{solid\ rock}$ = 165 m, W/$H_{solid\ rock}$ = 1.5), (**b**) Vertical section across panel, (**c**) Plan view, (**d**) Vertical section along panel ((**a**) Courtesy Gordonstone Colliery; (**b**), (**c**) and (**d**) after Hatherly and Luo 1999)
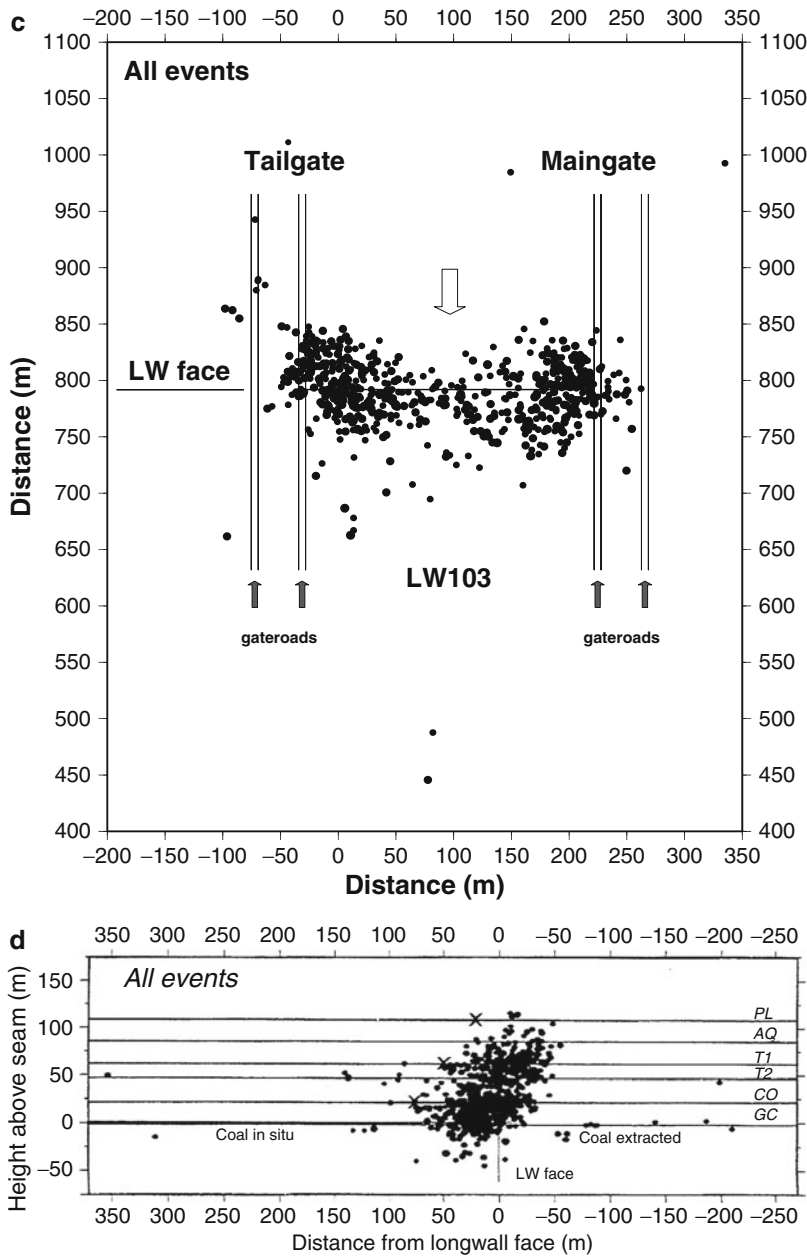
Fig. 3.18 (continued)

readily caves, there is considerable scope to apply the abutment angle concept.

The ground behaviour at Gordonstone Colliery contrasted with that monitored at the much deeper Appin Colliery. Appin Colliery extracted a 2.3 m thick seam at a depth of about 500 m utilising a 200 m wide longwall face, resulting in individual panel width-to-depth ratios, W/H, of only 0.4–0.5. The superincumbent strata comprised an alternation of sandstone units up to 120 m thick with interspersed claystone and shale units up to 25 m thick. This strata was described in general terms as constituting medium to strong roof conditions (Kelly
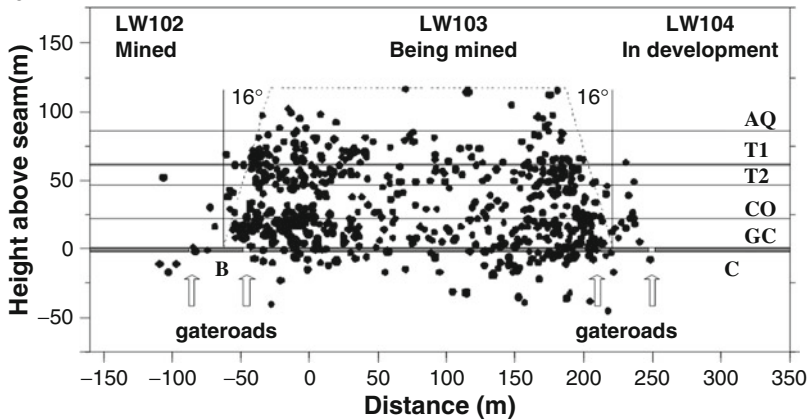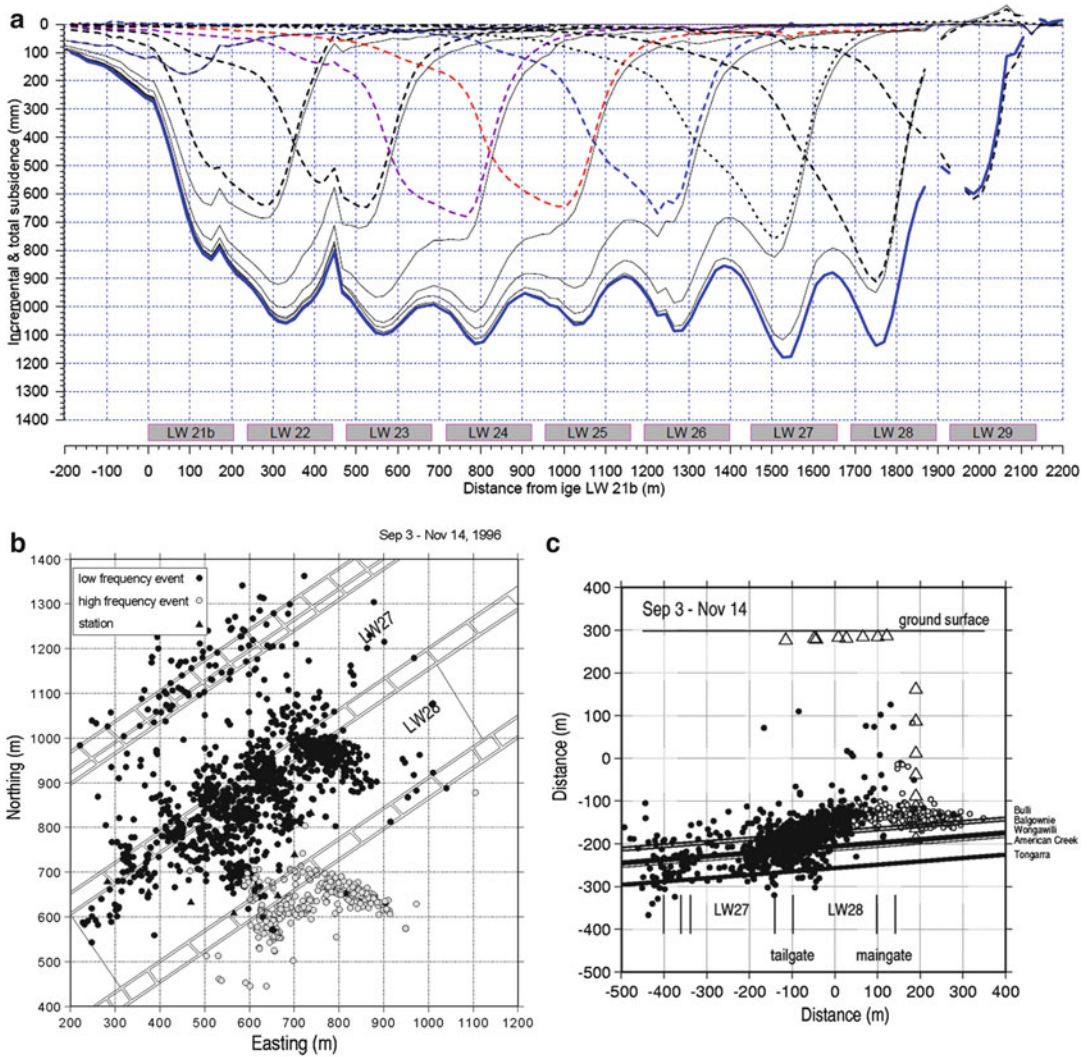
Fig. 3.19 Surface subsidence profile and microseismic event location plots associated with extracting LW 28 at Appin Colliery. (**a**) Transverse incremental and total vertical surface displacement profiles ($H_{solid\ rock}$ = 410 to 455 m, $W/H_{solid\ rock}$ = 0.45 to 0.5), (**b**) Plan view, (**c**) Cumulative events in vertical plane ((**a**) Adapted from MSEC 2007; (**b**) and (**c**) after Hatherly and Luo 1999)

et al. 1998). Figure 3.19 shows how vertical surface displacement developed incrementally in these circumstances. Microseismic activity in the floor was biased towards the tailgate of the active longwall (Longwall 28) but also occurred beneath the tailgate of the previously extracted panel. Microseismic activity was also detected on a geological structure some 400 m ahead of the face. The microseismic monitoring identified cyclical caving behaviour, evident from

Fig. 3.19b, with failure still tending to occur ahead of the face.

The profiles of vertical surface displacement and the biased nature of the microseismic activity at the Appin Colliery research site reflect that in subcritical panel width-to-depth situations, abutment load on interpanel pillars develops incrementally at moderate to large depths of mining as the stiffness of the superincumbent strata is reduced to zero during the course of extracting

several panels. In other words, there is considerable interaction between adjacent workings. The abutment angle concept fails to encapsulate this behaviour.

The two preceding caving behaviours fall towards either end of the spectrums for mining depth and total extraction panel width-to-depth ratio. They contrast with that associated with panels of subcritical panel width-to-depth ratio in a layout where, because of shallow depth and/or relatively wide interpanel pillars, caving does not fully develop and is not significantly impacted by the extraction of subsequent panels in the series. That is, surface subsidence does not develop incrementally to any significant degree as the overall extent of extraction increases. Microseismic monitoring indicates that in these instances, failures are concentrated behind the face, rather than ahead of the face, and are predominantly tensile failures rather than shear failures (Frith and Creech 1997; Strawson and Moodie 2007).

The shape of curves showing panel width-to-depth ratio, W/H, plotted against vertical surface displacement for isolated panels, such as those shown in Fig. 3.14, reflect the fact that there is a transition rather than a step change between subcritical and supercritical caving behaviour. The magnitude of load transferred onto the abutments of an excavation is determined by the extent of subsurface caving and fracturing and, as reflected by Fig. 3.14, this may be more complex to calculate than simply invoking the concept of an abutment angle.

The increase in stiffness of the superincumbent strata with depth and the impact that this has on interpanel pillar load is reflected, for example, in experience with the two chain pillar design procedures, Analysis of Longwall Pillar Stability (ALPS) and Analysis of Longwall Tailgate Serviceability (ALTS). Abutment angles for these two design procedures vary across a broad range that includes 21° as reported by Mark (1992) for USA sites; 5.1°–24.7° deduced from stress measurements in Australia by Colwell (1998); and 11.5° at a depth of 530 m in Australia as reported by Moodie and Anderson (2011). In the case of Australian operations, it was reported that departure between the proposed ALPS pillar loading cycle and the monitored chain pillar loading behaviour was particularly evident for the deeper mines with low panel width-to-depth ratios and 'bridging' strata. Colwell (1998) also reported that some concern has been expressed in the USA that the chain pillar design methodology, ALPS, 'does not work very well' at deep cover with particularly strong ground conditions.

Vandergrift and Conover (2010) report that it has been speculated that ALPS overestimates the load transferred to the gateroads under deeper cover. The authors advise that instrumentation data from a geotechnical program conducted at a depth of ~420 m to ~535 m appears to indicate that load-transfer to the gateroad pillars is less than previously assumed on the basis of ALPS and that this may help explain why gateroad pillars with relatively low calculated stability factors have performed adequately at that mine site. The researchers calculated abutment angles in the range of 3°–16°.

Similarly, the manner in which the transferred load is distributed within abutments is also a variable as it is influenced significantly by the stiffness and deformation properties of the immediate roof strata, coal seam and floor strata. For all other factors being constant, the location of the peak abutment stress moves further into the solid as the stiffnesses of the immediate roof, coal seam and floor strata decrease. Nevertheless, although abutment stress magnitude and distribution are variable, a number of empirical formulations have been developed that prescribe abutment stress distribution. Equations 3.10 and 3.11 are two which have found extensive application. Equation 3.10, proposed by Peng and Chiang (1984), defines the lateral extent of the side abutment zone, D, on the basis of depth of mining. Equation 3.11, proposed by Mark and Bieniawski (1987), defines the rate of decay of abutment stress in this side abutment zone.

$$D = 2.84\sqrt{3.3H}\,(m) \qquad (3.10)$$

where

$D = $ *lateral extent of side abutment zone (m)*

and

$$\sigma_{ax} = \frac{3L_s}{D^3} k (D - x)^2 \qquad (3.11)$$

where

$\sigma_{ax} = $ *abutment stress at distance x from the edge of the excavation*

$L_s = $ *total side abutment load based on abutment angle concept*

These types of relationships can be quite useful for making first pass assessments of abutment stress magnitudes and distributions. However, based on a consideration of applied mechanics principles, they cannot be expected to find universal application because they have no regard to the stiffness of the mining system. For example, as depth of mining increases, it is inevitable that panel width-to-depth ratio moves from being supercritical to being subcritical. This results in the formation of a bridge of superincumbent strata, the stiffness of which is not accounted for in the concept of abutment angle. Once a bridge is formed, the weight of the bridging strata (which determines abutment stress magnitude) increases in direct proportion to the thickness, t_b, of the bridge, while the stiffness of the bridging strata (which determines abutment stress distribution profile) increases in direct proportion to the cube of its thickness; that is, $(t_b)^3$. Subsequently, back-analysis of USA and Australian in situ stress data by Tulu and Heasley (2011) has confirmed that measured abutment stress magnitude and extent can deviate significantly from the values predicted by Eqs. 3.10 and 3.11 and that a range of additional parameters need to be incorporated into these formulations.

Pressure burst events provide further evidence of the variation in abutment loading with overall width of extraction at depth. For example, Agapiot and Goodrich (2000) reported on the extraction of 200–250 m wide longwall panels at a depth of 600 m in Utah, USA, in which pressure bursts only became significant after the third panel had retreated a distance of 460 m.

Abutment stress generation and distribution is more complex when considering behaviour in the corners of an extraction panel and requires a three-dimensional perspective. As the corners are approached, the in situ support to the undermined strata increases and the strike direction of fracturing associated with caving has to rotate through 90°. These changes can result in both a reduction in the dip of mining induced stress fractures and an increased bridging of strata across the corners of the excavation. The extent of these changes is dependent on the depth of mining, panel width-to-depth ratio, the nature of the immediate roof, and the width of the interpanel pillars.

Figures 3.12 and 3.20 illustrate some of these aspects. In the former case, the immediate roof strata was weak and bedded, with caving extending into the corner of the longwall panel at a relatively steep angle. In the latter case, the longwall panel had only recently commenced and full caving was yet to be established. The roof was stronger and not as bedded, resulting in caving developing at a much flatter angle and not extending into the corners of the panel.

Numerical modelling now offers significant benefits for quantifying stress magnitudes and distributions about total extraction panels. Examples include Fig. 3.21 and the numerical modelling studies reported by Salamon (1991a), Gale (2004), Peng (2008) and Esterhuizen et al. (2010b).

3.3.2 Strong Massive Strata

In geology, the term **massive strata** is used to describe a rock mass that has a paucity of well developed bedding planes. Although the term has been ascribed a variety of definitions in ground engineering (reference, for example, Wilson (1986), Frith et al. (1992b), MDG-1017 (1994), Singh (2000) and Gale (2009)), these generally capture this intent. In respect of caving behaviour over coal mine workings, the term has come to be associated with strata that have a capacity to span considerable distances and impede the development of subsurface subsidence and, consequently, goaf consolidation and vertical

Fig. 3.20 Caving
behaviour of moderately
strong, bedded roof strata at
the gate-end of a longwall
panel during the early
stages of retreat

Fig. 3.21 Stress
magnitude and distribution
about a longwall layout as
determined by numerical
modelling (After ACIRL
1984)
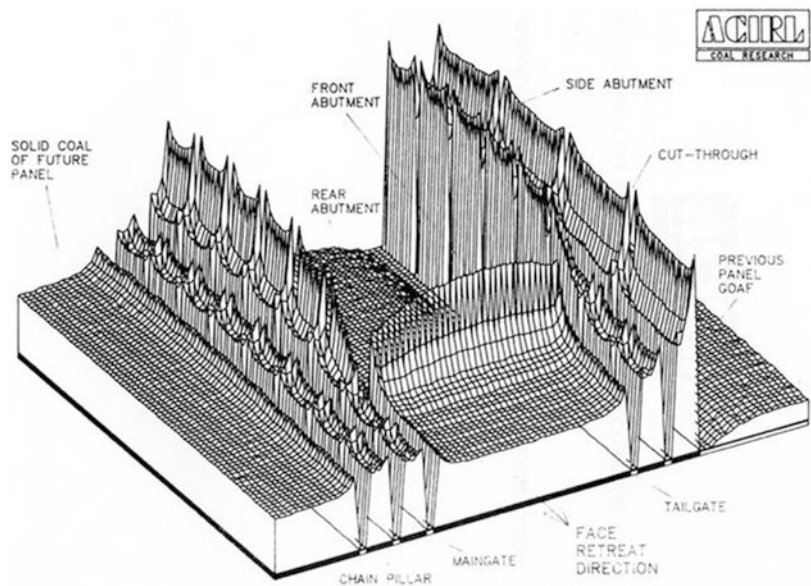
surface displacement. The spanning capacity of individual stratum increases with increase in their stiffness. In turn, stiffness increases with increasing stratum thickness, which is a reflection of how massive the stratum is, and with increasing elastic modulus, which has some imprecise correlation with strength. Hence, in the underground coal mining sector, the term 'massive' is often used loosely to refer to strata that are strong and have a capacity to span. These strata are not always massive in the strict geological meaning of the term. They most often comprise sandstones, conglomerates, limestones and dolerite sills.

Another legacy in the underground coal mining sector is to refer to strata as 'competent'. This term is not formally defined but to a coal miner, it generally implies that the rock mass is structurally stable and capable of spanning with minimal supplementary support in the given circumstances. This use of the term is scale dependent. For

example, roof strata classified as 'competent' in a roadway might be considered 'incompetent' in the centre of a pillar extraction or longwall panel.

The reader needs to be alert to these terminological legacies and may sometimes need to deduce for themself what the terms 'massive' and 'competent' are intended to convey regarding rock mass properties. This text has endeavoured to avoid the use of the term 'competent' and to use the term 'massive' in accordance with its geological meaning. However, in some instances it has had to adopt the terms as used in published literature.

Dolerite sills have been implicated in a number of ground instabilities in first workings, pillar extraction and longwall mining, the most notable being the sudden collapse of Coalbrook Colliery in South Africa in 1960 (Moerdyk 1965) and the dynamic weighting of the longwall face at Churcha West Colliery in India in 1990 (Gupta and Ghose 1992). Their behaviour has been studied in detail in South Africa and provides a well researched point of reference for understanding the behaviour of massive strata. The sills are typically 30–70 m thick and are capable of bridging spans measured at their base of well in excess of 100 m, with associated vertical surface displacement of less than 300 mm (Galvin 1982). This is despite the presence of ubiquitous vertical, and to a lesser extent, horizontal cooling joints, as illustrated in Fig. 3.22. The lack of bedding planes in the material and its high intact strength are illustrated by the length of recovered core in Fig. 3.23. The base of this core had broken on a drilling induced fracture.

Salamon et al. (1972) applied a simple elastic thin plate model to estimate the span required to break a dolerite sill. The model was refined by Galvin (1981) to take account of the parting thickness between the coal seam and the base of the dolerite sill, the angle of caving of this parting, and the effect of overburden stiffness on surcharge load. This resulted in derivation of the formula given by Eq. 3.12 for calculating the minimum mining span required to induce failure of a dolerite sill.

$$W_m = \sqrt{1165t_d - 935\frac{t_d^2}{D_d} + 2t_p cot\beta} \quad (3.12)$$

where

Fig. 3.22 An example of the structural fabric of a dolerite sill after it has been impacted by blasting in a quarry (After Galvin 1982)

$W_m =$ minimum span at mining horizon required to break sill

$t_d =$ thickness of dolerite sill

$D_d =$ depth to base of dolerite sill

$t_p =$ caving angle in degrees measured from the mining horizon

$\beta =$ caving angle in degrees measured from the mining horizon

This formula has been applied extensively and with considerable success (Wagner 1994; Latilla and van Wijk 2003), albeit that it is a two-dimensional model applied to what is essentially a three-dimensional structure. Figure 3.24 shows how the maximum stress at the base of an elastic plate develops with face advance, L. Of practical importance is that the maximum stress acting in the base of a plate changes insignificantly once face advance exceeds 2.5 times the panel width. Hence, if failure of a

Fig. 3.23   A length of core recovered from a dolerite sill illustrating the lack of bedding planes in the material and its high intact strength (After Galvin 1981)

Fig. 3.24   Development of maximum stress at the base of an elastic plate as a function of the ratio of face advance to panel width (Adapted from Galvin et al. 1981)

massive stratum has not occurred by that stage and geological conditions do not deteriorate, it is unlikely to occur with further face advance.

In addition to generating elevated abutment stresses, the presence of an unfailed massive bed in the superincumbent strata of an extraction panel can result in an increase in the lateral extent of elevated abutment stresses. This response is not captured in empirical formulae for abutment stress distribution that are based only on depth of mining, such as that defined by Eq. 3.10. Both effects can cause serious stability problems at the mining face and in flanking roadways, panel pillars and interpanel pillars in the lead up to the initial failure of the massive strata and, if it does not break, for the life of the panel. One control implemented in these circumstances in total extraction operations in South Africa and Australia is to reduce panel width, typically from the order of 200 m back to 100–130 m (Henderson 1980; Galvin et al. 1982; Beukes 1989; Frith and Creech 1997) and to leave substantial pillars between panels.
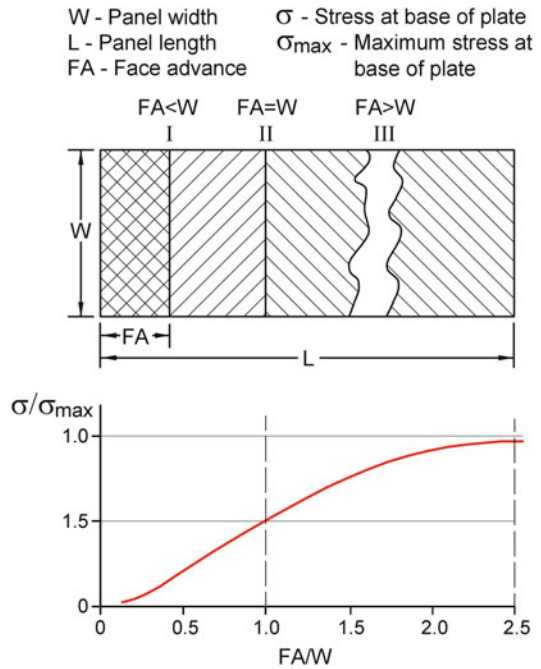
Failure of a massive stratum effectively unclamps only one of the four edges of the plate and so the stratum still has a capacity to cantilever off the face line for a considerable distance into the goaf before failing, thereby generating high abutment pressures on a cyclical basis. The bridging of a massive stratum also results in the caving and subsidence process being interrupted, causing a cavity to form beneath the massive stratum and, thus, discontinuous subsidence. If the bridging stratum is within the caving height, h_c, caving will cease before the goaf is choked due to bulking. If it is higher in the roof, subsidence of the underlying strata will result in a gap beneath the massive stratum, as illustrated in Fig. 3.25. Depending on mining height and parting thickness, this gap could range from hundreds of millimetres up to several metres. The formation of a gap can give rise to windblast, gas inrush and water inflow hazards in the event of failure of the massive stratum.

On the basis of elastic plate theory, once flexural fracturing of a massive stratum is initiated, it should result in an increase in bending stress in the remainder of the stratum, thus causing
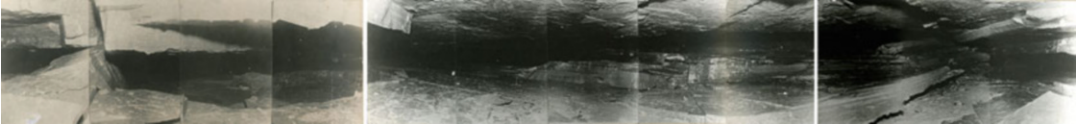
Fig. 3.25 A 360° view of a 300–700 mm wide gap within a dolerite sill associated with discontinuous subsidence (Courtesy of Professor Miklos Salamon)
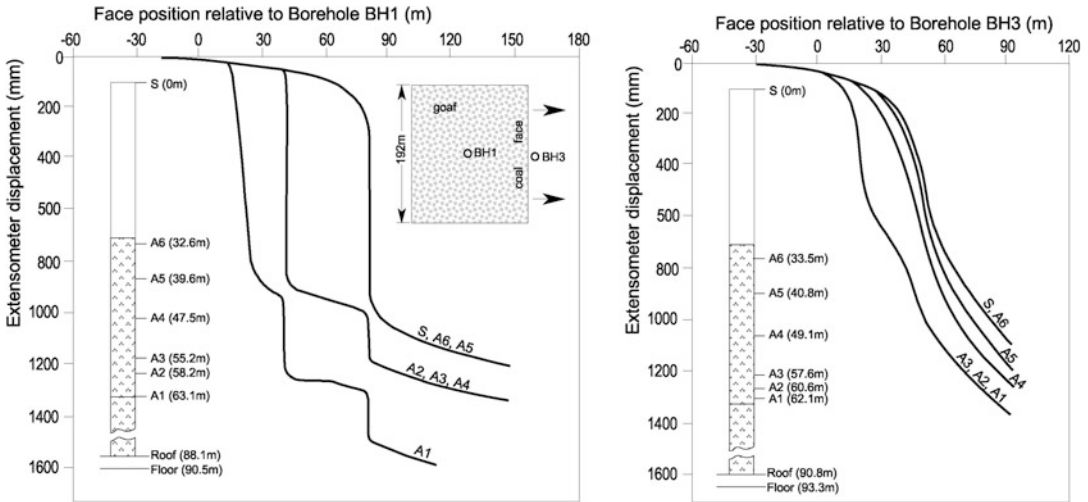

Fig. 3.26 Graphs showing progressive step-failure of a dolerite sill as recorded using surface-to-seam borehole extensometers (Adapted from Salamon et al. 1972)

fracturing to propagate rapidly through the rock mass. However, field measurements in South Africa have revealed that this failure process may develop in a number of distinct steps that are dependent on further increases in the minimum panel span (Galvin 1983). Field observations indicate that similar behaviour can occur in massive conglomerate/sandstone stratum in Australia. Gupta and Ghose (1992) concluded that the dynamic periodic weighting accident at Churcha West Colliery in India, which destroyed 23 longwall hydraulic face supports, was associated with failure of the lower 19–30 m of a 125 m thick dolerite sill, some 85 m above the working horizon.

Figure 3.26 shows caving behaviour in a dolerite sill above a longwall panel in South Africa, as recorded using multipoint surface-to-seam extensometers. Subsidence terminated initially at the base of the sill and then progressed through it in two distinct steps. Immediately prior to full collapse, the longwall panel was bridged by a beam of dolerite that was somewhere between 7.6 and 15.5 m thick and supporting its own weight and that of 36 m of overburden. It has been suggested that the behaviour may be associated with the redistribution of horizontal stress as failure progresses through the massive strata, with the increased lateral stress improving the structural stability of the remaining jointed material (Galvin 1983). With subsequent advances in the rock mechanics knowledge base, it is possible that it may also be attributable to the formation of linear arches (voussoir beams).

Of particular significance in Fig. 3.26 is the small amount of surface subsidence up to the onset of the final collapse and the rate at which subsidence developed. Similar behaviour is associated with total extraction beneath massive conglomerate/sandstone strata in the Newcastle Coalfield, NSW, Australia. This behaviour illustrates how surface subsidence measurements

Fig. 3.27 Apparent abutment shear failure above a massive dolerite sill overlying a longwall panel. (**a**) Steep step in surface profile at the perimeter of the subsided plug. (**b**) Overall view of subsided plug (After Galvin 1981)
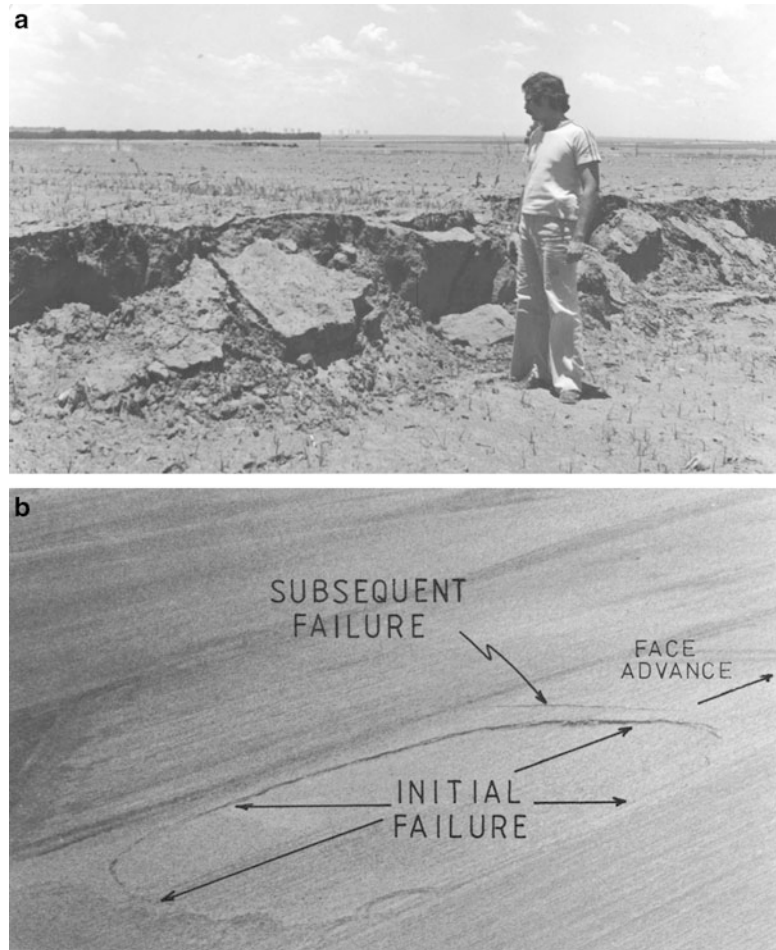
can be a poor indicator of the overall state of caving and stability of a massive strata. Therefore, it is advisable in sensitive or critical situations to monitor subsurface behaviour with extensometry. Field observations also reveal that, on occasions, the final failure of massive strata may be associated with shear failure at the panel abutments, shown in Fig. 3.27, which is not inconsistent with the plug failure model of Galvin (1982b) or with the failure of a linear arch.

Three potentially serious hazards associated with total extraction mining beneath massive strata are excessive abutment stress throughout the operating life of a panel, periodic weighting, and windblast. From an operational perspective, it is desirable to make a panel sufficiently wide to induce failure of massive strata as soon as possible after the commencement of mining.

Alternatively, the panel span needs to be restricted so that caving does not occur and abutment stresses are not excessive. A situation to be avoided is where the panel span is only marginally less than the critical span, such that mining operations are subjected to high abutment stress for the operational life of a panel and prone to a small change in geology triggering the collapse of a large area of strata within the goaf. This latter situation creates the potential for the ingress of flammable and noxious gases into the workplace and for windblast.

If panel span is insufficient to induce full caving of the superincumbent strata, then careful consideration has to be given to the separation distance between panels. This is to avoid both exposing subsequent operations to high abutment stress and exposing personnel to an inrush or

windblast caused by the collapse of a large area of standing goaf in the previously extracted panel.

In some situations, a massive rock mass may fail in stages in a rapid but not uncontrolled manner. Hardman (1971) reported that of a total movement of 700 mm in the lower half of a dolerite sill when it failed, 530 mm occurred within a period of about 1 min. Gupta and Ghose (1992) reported that 1500 mm of leg closure was recorded in less than 1 h in the incident attributed to the catastrophic failure of the base of a dolerite sill in India. Total extraction beneath massive conglomerate strata in the Newcastle Coalfield of NSW is well known for resulting in sudden and dynamic failures of the conglomerate that generate severe windblasts (see Sect. 11.1) It is noteworthy that the consequences of failure of massive dolerite sills in South Africa have not been as severe as the failure of massive strata in Australia. This appears to be due to adherence in South Africa of the advice of Salamon and Oravecz (1976). They advised that it would be prudent to provide a protective cushioning to a failing dolerite sill by restricting total extraction to areas where the normal shale/sandstone parting between the dolerite and the seam was not less than 8–10 times the mining height.

3.3.3 Span Design

So-called 'first working' mining systems in coal mining are based on bord and pillar mining in which coal extraction is confined to relatively narrow roadways that define coal pillars whose purpose is to maintain the integrity of the superincumbent strata. As the depth of mining increases, percentage extraction rapidly drops in these mining systems because of the need to leave larger pillars to support the increased weight of the overburden. Hence, subject to safety and environmental considerations, mining usually reverts to some form of secondary extraction in which coal pillars are subsequently extracted to form wide excavations. These secondary extraction mining methods are loosely referred to as 'total extraction' mining methods

and are dominated by pillar extraction (discussed in Chap. 8) and longwall mining (discussed in Chap. 9).

The determination of panel span in total extraction situations is a site-specific matter since it is a function, amongst other things, of the composition, thickness, depth and relative position of the various stratum that make up the overburden. Design can be aided considerably by prior operational experience in the given or similar conditions.

The formation of a secondary extraction panel can give rise to high abutment stresses. While considerable research has been undertaken into quantifying abutment stress distributions about longwall entries, or gateroads, and developing design and support procedures for controlling the impacts of this abutment stress on these roadways, the same is not the case for managing impacts on the mining face. Ideally, mine design should result in either:

- an excavation span (width) that is sufficiently wide so as to induce full caving and subsidence of the overburden very soon after the commencement of secondary extraction in order to maximise relief from abutment stress; or
- an excavation span that is sufficiently narrow so as to restrict abutment stress.

In practice, this can be a complex design exercise. Not only is face abutment stress indeterminate because it is a function of the stiffness of the mining horizon and of the surrounding strata, but also in secondary extraction situations the stiffness of the surrounding strata is also governed by the caving and subsidence behaviour of the overburden and the reconsolidation characteristics of the goaf. The situation becomes more challenging as depth increases because face abutment stress is determined increasingly by the degree of interaction between panels, as reflected in the variation in the profiles of vertical surface displacement shown in Figs. 3.14, 3.15, 3.16, 3.17, 3.18, and 3.19. Neither ideal span designs may be achievable at depth, simply because they result in

spans that are either too small to be economically viable or too large to be practically achievable.

In addition to abutment stress, span design may need to take account of a range of other factors, three of the more important being wind-blast (see Sect. 11.1), subsurface subsidence impacts (see Sect. 10.3), and surface subsidence impacts (see Sect. 10.4). Often, these are the primary determinants of panel span, with their control usually resulting in panel span having to be restricted to a subcritical width. Many serious incidents have been associated with this approach when panel span has been only marginally less than that required to induce full caving. In these situations, the extraction line may be subjected to high abutment stress throughout the life of the panel; ground control can be very susceptible to small changes in geology; rib spall may be severe; and localised caving may occur on an irregular basis. Hence, strata behaviour is inconsistent and unpredictable. These situations serve as examples of where the controls introduced to mitigate one risk can introduce new and sometimes higher risks. This is why it is essential that risk management controls are also risk assessed in their own right (see Chap. 12).

A number of different methodologies are utilised in practice to select panel span. None are universally applicable and all have strengths and weaknesses. These methodologies include:

- Experiential, usually developed out of trial and error. This approach is epitomised in pillar extraction, where there is a multitude of variations in extraction technique and panel span and strong regional preferences for certain variants and mining dimensions.
- Empirical. There is a variety of empirical approaches, with the oldest and most extensively applied being based on observations of vertical surface displacement above isolated total extraction panels. These observations are often presented in the form of dimensionless plots, such as that shown in Fig. 3.14, by normalising panel span, or width, with respect to depth and plotting this ratio against vertical

displacement normalised with respect to mining height. The variety of curves shown in Fig. 3.14 mainly reflects the different site-specific geomechanical conditions. The curves display the same generic trait of vertical surface displacement increasing gradually with increase in excavation width-to-depth ratio, W/H, then accelerating through a transition zone, before reaching a peak value at a width-to-depth ratio of around 1–1.2.

These type of curves provide insight into the state of caving about a total extraction panel and can assist in deducing the state of abutment stress. However, limitations are associated with them, including that they can mask discontinuous subsidence situations and do not reflect increasing interaction between panels as depth of mining increases for a given panel width-to-depth ratio, W/H. This latter limitation can be overcome to some extent by computing the increment in vertical displacement associated with the extraction of each panel. Figures 3.16 and 3.19 are examples of this approach. Plots of incremental subsidence give better insight in the development of abutment stress but deductions still have to be made regarding abutment stress magnitude and distribution.

Empirical formula such as those defined by Eqs. 3.10 and 3.11 and variants of these developed for pillar extraction situations (such as the Analysis of Retreat Mining Pillar Stability Methodology (ARMPS) (Mark et al. 2011)), provide an alternative means for estimating abutment stress magnitude and distribution that do not depend on local knowledge or experience. Nevertheless, these types of approaches are still constrained by an inability to fully consider the stiffness of the loading system.

It has been suggested by some researchers that the mining rock mass rating system (MRMR) as developed and applied by Laubscher (1994) to predict the caveability of superincumbent strata could find application in coal mining situations. Although a number of coal mine sites are included in the

database that underpins this rock mass classification system and its subsequent iterations, this approach has found very limited application in the coal sector to date.

Empirical approaches to panel design predominate in situations where the undermining of strong and massive stratum can give rise to the risk of windblast. A number of mines in the Lake Macquarie region of Australia developed their own panel span criteria for extracting coal pillars directly beneath a massive and strong sandstone/conglomerate roof strata in the Great Northern Seam (personal experience). Frith and Creech (1997) developed an empirical relationship for designing panel width to mitigate face instability when longwall mining directly under similar strata in the northern region of Lake Macquarie. While the procedure proved successful for preventing very large rib falls that then gave rise to large roof falls, the associated reduction in panel width resulted in violent windblasts that, arguably, presented a greater risk to personnel than the risks associated with falls of rib and roof that the procedure was intended to mitigate.

- Semi-empirical. Generally, this approach is based on simple analytical models that have been refined and calibrated using empirical data. The Galvin dolerite span formula, given by Eq. 3.12 is one such approach. This formula has been in use for over 30 years and has served the South African mining industry well in determining the mining spans required to induce full caving of dolerite sills. Nevertheless, reliance still has to be placed on operational experience in assessing if tolerable abutment stress conditions are likely to be associated with the calculated critical span. Because the formulation was derived on a database specific to the behaviour of dolerite sills in South Africa and is not mechanistically rigorous, it does not find universal application, although it has provided good approximations in some situations associated with strong and stiff sedimentary strata.
- Analytical. Linear arch theory (Sect. 2.8.8) finds application in both civil and mining

engineering practice in calculating spanning capacity (reference, for example, Beer and Meek 1982; Wold and Pala 1986; Pells and Best 1991; Nomikos et al. 2002; Seedsman 2004; Brady and Brown 2006). However, these applications are primarily focussed on assessing spanning capacity and vertical surface displacement and do not provide an assessment of abutment stress magnitude and distribution in and about a mining face.

- Numerical. In theory, numerical modelling offers the significant benefit of being able to take account of the stiffness of the loading system and, therefore, to produce abutment stress magnitude and distribution profiles around the full perimeter of an excavation, as illustrated in Fig. 3.21. However, in practice, considerable uncertainty can be associated with the accuracy of input data, especially in regard to caving and goafing characteristics. Limitations are associated with three-dimensional numerical modelling, especially when attempting to simulate some pillar extraction layouts.

In summary, surface subsidence observations provide insight into the state of abutment stress and provide a sound basis for testing the validity of numerical models. Semi-empirical and analytical models can provide reasonably accurate estimates of the span required to induce full caving and subsidence if calibrated to site-specific data. Some also produce abutment stress magnitude and distribution profiles but care is required when these models are applied to situations that fall outside the site-specific conditions for which they were derived. Numerical models can be very helpful for quantifying abutment stress magnitudes and distributions as a basis for selecting mining span. However, they may also be unreliable and, therefore, outcomes should be used as an aid and supported by parametric and sensitivity analysis, rather than being accepted blindly as accurate simulations of reality. Irrespective of the desktop approach taken to design, local operational experience is generally invaluable when determining mining span.

3.4   Elevated Horizontal Stress

Underground coal mining often takes place in environments where the major principal stress is horizontal. The adverse impacts of high horizontal stress on weak, bedded and laminated roadway roof and floor strata can be avoided by orientating roadways parallel to the direction of the major horizontal principal stress. However, this is rarely possible for many reasons. Stress direction can change across the mining lease, in the vicinity of geological structures, and beneath topographic highs. In any case, roadways still need to be connected at regular intervals by cut-throughs. Practical considerations such as lease boundaries, surface constraints, and seam dip also influence roadway direction. Roadway direction relative to seam dip, for example, has implications for water management, ventilation control, and equipment stability. In some cases, the minor horizontal principal stress may also be of sufficient magnitude to adversely impact roadway stability. Hence, compromises have to be made and it is almost inevitable that at some stage in the mining cycle, roadways will have to be developed at an angle to the major horizontal principal stress direction.

Figure 3.28 is an example of a streamline model that has found extensive application in elevated horizontal stress situations in coal mining to account for poor ground conditions biased to one side of the mining face, with this side varying with the direction of mining. It shows conceptually and correctly how in-seam horizontal stress is redistributed ahead of, under and over the face of a roadway that is advancing at an acute angle to the direction of the major horizontal stress. The poorer roof conditions, guttering and floor heave encountered on the 'leading corner' of roadways in elevated horizontal stress situations have often been attributed in the past to in-seam stress redistribution being concentrated about that point.

Although the model correctly predicts the site of most impact, attributing the impact to the redirection of in-seam stress is questionable in the case of underground coal mining. This is

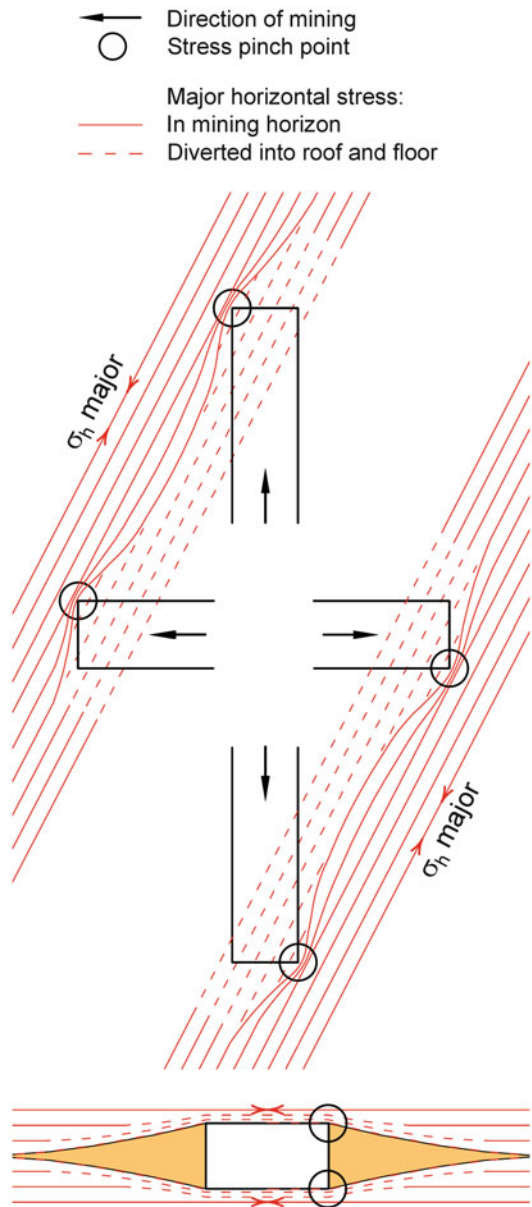**Fig. 3.28** An example of a widely adopted and now highly questionable streamline model to account for biased adverse roof and floor conditions in a high horizontal stress field in an underground coal mining environment

because it is generally the case that coal seams are not subjected to high horizontal stress (see Sect. 2.6.7). The in-seam stress that is redistributed into the roof and floor strata may

aggravate a state of instability but, because of its low magnitude, this stress is very unlikely to be the primary cause of the poor roof and floor conditions.

The biased face conditions in coal mining are most likely attributable to a reduction in confinement to the immediate roof and floor strata. As the roadway is advanced, the normal stresses acting on the immediate roof and floor strata are removed, whereas the horizontal stresses acting in the immediate roof and floor strata remain high and may increase slightly due to the redistribution of the in-seam stress. This changed state of stress creates a high propensity for buckling and flexural (bending) failures of roof and floor strata, especially in bedded or thinly laminated strata. Softening and failure of roof and floor strata around the leading corner of a roadway effectively creates a stress relief slot (see Sect. 5.2.3) that then provides a degree of horizontal stress relief to the immediate roof and floor strata over the remaining width of the roadway.

In the case of the roof strata, the onset of failure and the extent of roof damage depend to a large extent on the magnitude of the horizontal stress field, the structural and strength characteristics of the immediate roof strata, the minimum distance that support and reinforcement can be installed from the face and the timing of the installation of these ground control measures. In very weak strata and/or high horizontal stress situations, the roof may gutter close to or at the affected face corner as excavation is occurring. Ground control largely depends on minimising the span between the face and the last row of installed ground support and on the effectiveness of this support system. It stands to reason, consistent with field experience, that there are benefits in these situations in installing ground support as soon and as close as possible to the face. This is to promote beam building; to mobilise the residual strength of failed strata; and to prevent unravelling and falls of ground, with additional reinforcement and support elements being installed on the affected side of the roadway in an endeavour to restore some degree of confinement.

In the seam horizon itself (ribsides and face), elevated horizontal and vertical stresses exist immediately ahead of the leading corner. As a result of roadway advance, the horizontal stresses acting normal to the ribsides and face will become zero whereas the tangential stresses acting in the ribside and face will remain relatively unchanged. The vertical stresses in the rib side and the face also do not change significantly as a result of roadway advance. Hence, these in-seam stress changes are not as pronounced as those that impact the immediate roof and floor strata. Against this background, it is suggested that the impact of high horizontal stress in the roof and floor strata is better conceptualised as shown in Fig. 3.29.

The problem is truly three-dimensional. Three of the roof beam abutments are clamped but the fourth has indeterminate end constraints. At and around the corners of the roadway, the principal stresses are not aligned with the roadway span or with the direction of roadway advance. Amongst other things, this causes shear stresses to act in these directions and between strata. These factors have important implications when attempting to calculate the stresses (and equivalent forces) that lead to roof and floor bending and buckling. Analysis of this environment and associated ground support and reinforcement requirements falls well outside the scope of simple beam theory.

It is essential when mapping roadway conditions for the purpose of interpreting stress direction that, as evident from Fig. 3.29, careful note is made of the direction from which the roadway was mined. When both sides of a roadway show signs of guttering, it is likely that either the roadway orientation is within 30° of being normal to the major horizontal stress direction or the minor horizontal stress is also elevated. Once a roadway is within 30° of being
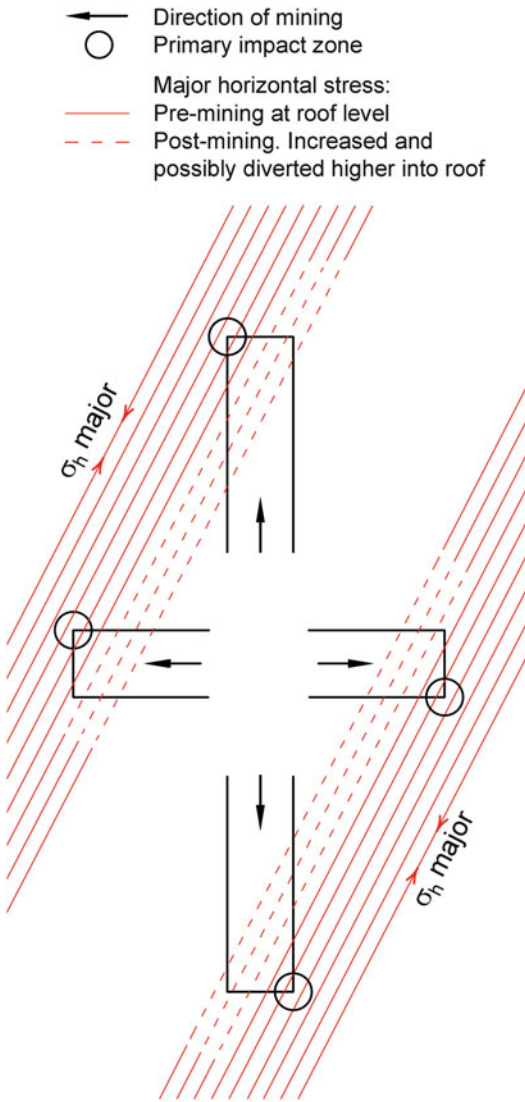
Fig. 3.29 A preferable model for determining the location of biased adverse roof and floor conditions in a high lateral stress field

parallel to the direction of the major horizontal stress, impacts tend to reduce rapidly with further decrease in this angle. Mine design and support measures for mitigating the hazards associated with elevated horizontal stress are discussed in more detail in Chaps. 7, 8, 9 and 10.

3.5 Shallow Mining

3.5.1 Principles

Analytical and numerical modelling confirm that at great depth, most of the rock surrounding a wide tabular excavation is subjected to compressive stresses. This means that the regional behaviour of the excavation is influenced little by geological discontinuities and is controlled mostly by the inter-relationship between the prevailing stresses and the mechanical properties of the rock, making it relatively easy to predict rock behaviour (Salamon 1983).

A similar situation can exist at shallow depth when the horizontal stress around an excavation is typically two or more times the vertical stress; that is, $k \geq 2$. However, the situation changes significantly as this stress ratio reduces and can present a very serious risk of unpredictable behaviour once the stress ratio is less than one. Even in a high horizontal to vertical primitive stress environment, these situations can arise at shallow depth in total extraction situations. This is because caving and subsidence disrupt the transmission of horizontal stress in the superincumbent strata, resulting in adjacent mining panels being located in a horizontally destressed environment.

A number of Australian and USA longwall operations have operated at depths as shallow as 18–50 m (Holt 1989; Frith et al. 1992a; Butcher and Kirsten 1999) while pillar extraction has occurred at depths at least as low as 30 m in South Africa (Schumann 1982) and 20 m in Australia (Enright 1995). As depth of mining decreases below about 100 m, and especially below 50 m, excavation behaviour becomes increasingly sensitive to small changes in geology, dimensions of the mine workings and field stress and, therefore, more unpredictable. In particular, as depth decreases:

- Geological features such as joints, faults and dykes are likely to be more weathered, open and continuous between the mine workings and

Fig. 3.30 Comparison of
tensile zones above and
beneath isolated total
extraction panels at shallow
depth and great depth for
k = 0.5 (Modified from
Galvin et al. 1982, after
Salamon 1974)
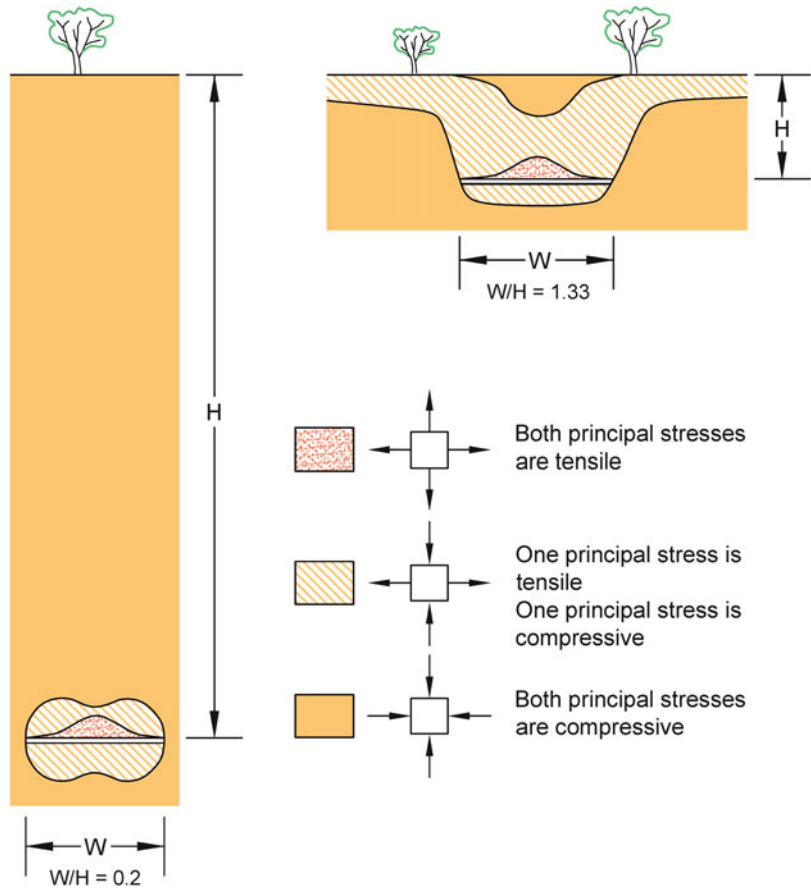
the surface. This increases the potential for
shear failure, which is elevated in wet weather
due to the reduction in effective normal stress
across potential sliding surfaces and, in some
circumstances, lubrication of these surfaces
(such as in some clay infill situations).

- The impact on overburden stiffness of unconsol-
idated surface deposits is proportionately
greater. This impact cannot be ignored at shal-
low depths, with the effective depth of (solid
rock) cover having to be reduced by a
corresponding amount and loaded with a
corresponding deadweight surcharge. In total
extraction mining at shallow depth, a small
increase in the thickness of unconsolidated over-
burden or in the overall span of the panel can
cause a large increase in the effective panel
width-to-depth ratio, resulting in both a signifi-
cant reduction in the overburden load trans-
ferred to the panel abutments and a significant

increase in the likelihood that any panel collapse
will be uncontrolled.

Elastic continuum numerical models provide
insight into overburden behaviour at shallow
depth, albeit that such models may not be repre-
sentative of the discontinuous nature of many
rock masses at shallow depth. Figure 3.30
shows the zones of principal stress about a shal-
low panel and a deep panel of the same width
predicted in this manner for a stress field in
which the horizontal to vertical stress ratio is
0.5 (Salamon 1974). The figure highlights that
the effect of a free surface on the stress distribu-
tion around an isolated panel cannot be ignored
once panel width-to-depth ratio exceeds 0.4. In
the shallow case:

- the vertical extent of the zone where both
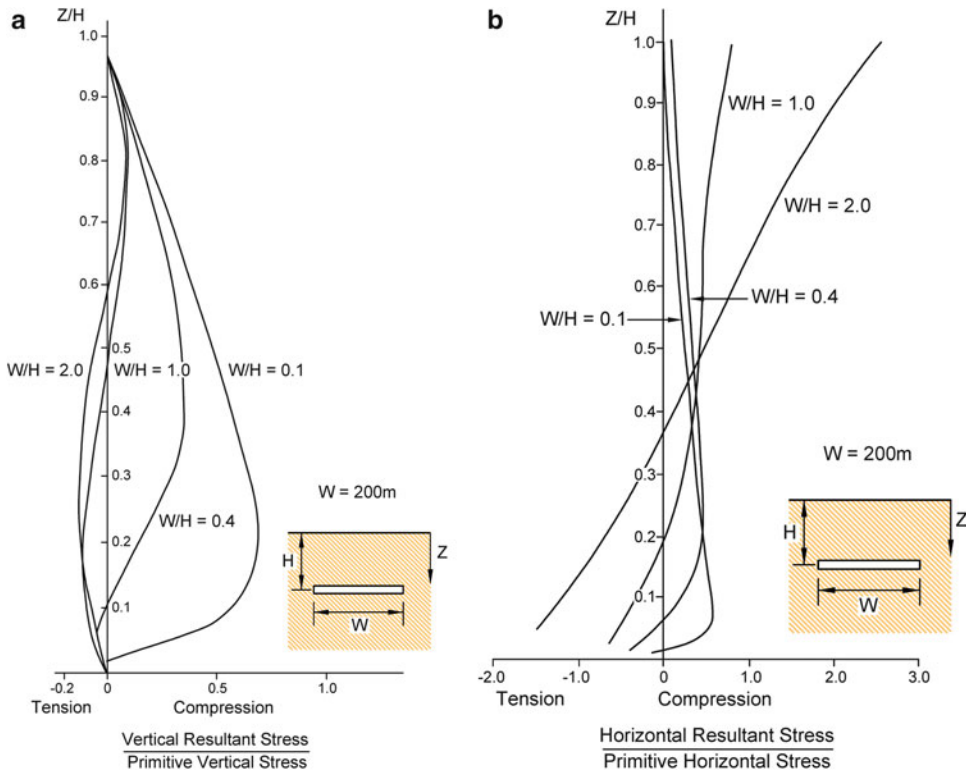principal stresses are tensile has increased;

Fig. 3.31 Normalised total vertical and horizontal stress above the centre of an isolated panel for various total extraction panel width-to-depth ratios, W/H, for

k = 0.5. (**a**) Normalised total vertical stress. (**b**) Normalised total horizontal stress (Modified from Galvin et al. 1982 after Salamon 1974)

- the zone where one of the two principal stresses is tensile extends right through to surface and outside the vertical projection of the panel; and
- an isolated zone where both principal stresses are compressive exists above the panel.

The total vertical stress (normalised with respect to primitive vertical stress) above the centre line of a panel for various values of panel width-to-depth ratio, W/H, for the case of k = 0.5 is shown in Fig. 3.31a. As depth of mining decreases, an increasingly larger proportion of the strata between the roof of the excavation and the surface is subjected to tensile stresses. In fact, from the stage when the span is equal to the depth, the vertical stresses are tensile in the lower half of the overburden. Similarly, the proportion of the roof strata where the horizontal stresses are tensile increases with increasing panel width-to-depth ratio (Fig. 3.31b).

The following important conclusions can be drawn from Fig. 3.31:

- The low tensile strength of rock and the presence of many structural weaknesses in the rock mass, such as bedding and joint planes, become significant features in the presence of extensive zones of tensile stress. Caving of the roof strata right through to the surface is a distinct possibility, particularly if the overburden comprises weak and friable rock.
- Only massive, strong rock beds are likely to remain unfractured once panel width exceeds twice depth (W > 2H).
- The tendency of the roof strata to cave through to the surface increases with increasing values of panel width-to-depth ratio.
- The existence of a continuous zone of tensile stresses from the surface through to the underground workings creates potential paths for the inflow of surface water.

Fig. 3.32 An example of a watercourse breaking through into shallow pillar extraction workings during a rainfall event

- Zones of high tensile strain and zones of high compressive strain are to be expected on the surface as a result of mining wide panels at shallow depth.

A second type of caving failure at shallow depth is that of **chimney caving** or **sinkhole** formation. In coal mining, these terms refer to failures of the roof strata over bords, particularly over intersections, that extend through to the surface. Sinkholes can increase the risk of spontaneous combustion of coal within the mine workings (because they permit the ingress of oxygen) and can present a risk to safety and the environment. The failures may develop as a plug but more often as falls of ground that progressively extend through to the surface. In the later case, bord width, mining height, bulking factor, depth, and the composition, competence and angle of repose of the superincumbent strata influence the development of a sinkhole. Canbulat (2003) has

provided an analytical model for evaluating these situations. Brady and Brown (2006) present a model based on limit equilibrium that finds application to shear failure in strong rock devoid of discontinuities. This type of behaviour is discussed in more detail in Chap. 10.

3.5.2 Practice

The ingress of rainfall into shallow total extraction workings is a common problem in underground coal mining due to the enhanced conductivity of the fractured overburden. With few exceptions, total extraction workings at shallow depth also result in wide surface cracks, sufficient to cause loss of water from natural and man-made storages and total loss of surface flow in watercourses. Surface water is diverted into the mine workings and/or downstream through sub-surface fracture networks

Fig. 3.33 Entrance to a shallow mine showing that almost 50 % of the overburden comprises a deadweight surcharge, hence resulting in roadways having a large effective panel width-to-depth ratio (W/H >3)

(see Sect. 10.3). Often, open fractures are remediated by ploughing, ripping and dozing. However, this process does not guarantee that fractures are sealed to any significant depth and it is not unknown for ephemeral water courses to break through into mine workings during flood events, such as shown in Fig. 3.32. A more permanent solution when fracturing is not extreme involves sealing the fractures with clay. In some cases, such as where oxygen ingress is to be prevented in order to control spontaneous combustion, this may require the placement of a clay blanket which, obviously, can have environmental implications.

In some shallow situations, a high panel width-to-depth ratio can be associated with a mine roadway, as in Fig. 3.33. When the thickness of the alluvium surcharge is taken into account, this mine entry has a panel width-to-depth ratio of the order of 3. In this example, stability was aided by the presence of a strong sandstone stratum some 3 m thick in the immediate roof. This was not the case for the situation shown in features Fig. 3.34. Due to the large mining height, weak superincumbent strata and

very shallow depth of mining, the sinkhole void in the latter case was very large and open to the mine workings, necessitating that it be backfilled. The backfilling method should be risk assessed for reasons apparent in Fig. 3.34. A more extensive layout of collapsed bords and intersections at shallow depth is shown in Fig. 3.35. Figure 3.36 shows the plug-like surface appearance of a fatal overburden failure event associated with pillar extraction at shallow depth.

The sensitivity at shallow depth of panel stability to small changes in geometry is demonstrated by considering a pillar extraction panel that has retreated 42 m without caving. The extraction of a 8 m wide pillar line (fender) from a 6 m wide roadway would result in the panel W/H ratio increasing by only 0.047 at a depth of 300 m but by 0.47 at a depth of 30 m. The impact of this change at shallow depth is illustrated by the case study shown in Fig. 3.37, in which pillar extraction at a depth of 30 m resulted in an open goaf measuring in excess of 70 m by 90 m. The production supervisor was fatality injured when, during the process of extracting a 6 m wide lift from the pillar, the entire area fell suddenly as a

Fig. 3.34 Intersection failure over thick seam bord and pillar workings at shallow depth

Fig. 3.35 Surface expression of a mixture of intersection falls and bord collapses over bord and pillar workings at shallow depth

plug to the surface, generating a large windblast. The supervisor had apparently positioned himself to watch for warning signs of a goaf fall, of which there appears to have been none.

The panel had commenced against a fault plane in order to encourage the early development of caving and it is thought that heavy rainfall leading to water ingress down the fault plane at the time of the incident was a contributing factor. Water ingress along geological structures is a known trigger for the failure of both pillars and excavations in all forms of underground mining. Wagner (1991), for example, reported that a reduction in the coefficient of friction on a fault plane due to the ingress of rainwater was a contributing factor to a regional collapse of chrome mine workings in South Africa.

Butcher and Kirsten (1999) provide a detailed appraisal of managing the risk of longwall extraction at shallow depth. The following potential hazards were identified on the basis of risk assessment:

- goaf hang up followed by sudden collapse to the surface;
- geological features parallel or sub-parallel to the face, resulting in sudden and severe loading of the face supports;
- sudden ingress of water or unconsolidated material from the surface;
- ingress of surface flood water during heavy rain and storms; and
- loss of ventilation through surface cracks, leading to possible spontaneous combustion events.

Actions and controls emanating from this risk assessment approach were:

Fig. 3.36 Surface expression of a sudden overburden failure event associated with pillar extraction panel at shallow depth
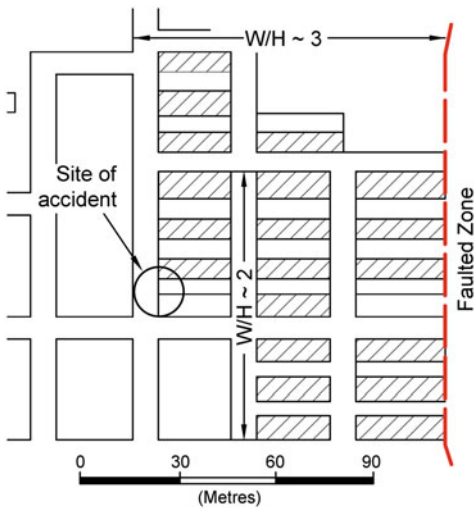
Mining height 2.4m.
Depth 20-30m.
Standing goaf > 60x90m.
Therefore minimum W/H>2.
No rib spall, roof sag, floor heave or
observable deflection of props prior to fall.
Mass vertical movement to surface.
Windblast.
Conditions excellent around edge after fall.

Fig. 3.37 Conditions associated with a fatal sudden collapse incident at shallow depth (Adapted from Galvin et al. 1994)

- thorough detailed geological mapping of gate roads and longwall face;
- extensometer monitoring of intersections and gateroads;
- in situ stress monitoring; (Aside: The effectiveness of this measure warrants careful consideration in shallow depth situations. The reliability and accuracy of the stress measuring equipment when installed in weathered rock may not be of an acceptable standard. In any case, stress and strain changes prior to the onset of instability may be low and may even fall within the sensitivity limit of the stress measuring equipment.)
- surface borehole extensometers when depth of cover was less than 35 m;
- regular monitoring and review of longwall support leg pressures and differential pressure between front and rear legs;
- monitoring face conditions each shear and implementing safety procedures immediately conditions fell outside a stated normal operating condition;
- daily surface subsidence monitoring;
- sealing of surface cracks along surface flow paths;

- additional surface inspections triggered by inclement weather to verify adequacy of surface diversions;
- emergency response and contingency plans.

These actions and controls were all encapsulated in a Shallow Mining Risk Management Plan supported by a Trigger Action Response Plan (TARP). This type of risk management approach is strongly advisable when undertaking secondary extraction at depths of less than about 50 m.

References

ACIRL. (1984). Stress distribution profile. *Coal Journal – Australian Journal Coal Mining Technology and Research* (3).

Agapiot, J. F. T., & Goodrich, R. R. (2000, August 8–10). *Five stress factors conducive to bumps in the Utah, USA, coal mines.* Paper presented at the 19th international conference ground control in mining, Morgantown, WV.

Beer, G., & Meek, J. L. (1982). Design curves for roofs and hanging-walls in bedded rock based on "voussoir" beam and plate solutions. *Transactions of the Institution of Mining and Metallurgy, 91*, A18–A22.

Beukes, J. S. (1989). *Considerations in the design and layout of pillar and rib pillar extraction panels.* Paper presented at the symposium on advances in rock mechanics in underground coal mining, Witbank.

Brady, B. H. G., & Brown, E. T. (2006). *Rock mechanics for underground mining* (3rd ed.). Dordrecht: Springer.

Butcher, R., & Kirsten, M. (1999, June 15–18). *Experience with very shallow cover longwalls, Baal Bone Colliery.* Paper presented at the 2nd international underground coal conference, Sydney.

Campoli, T. M., Barton, T. M., van Dyke, F. C., & Gauna, M. (1990). *Gob and gate road reaction to longwall mining in bump-prone strata.* Research investigation RI 9325 (pp. 38), U.S. Bureau of Mines.

Canbulat, I. (2003). Sinkholes and bulking factor analysis in coal mines. *South Africa National Rock Engineering News* (July), 1.

Colwell, M. G. (1998). *Chain pillar design – Calibration of ALPS.* ACARP end of grant report C6036 (pp. 116). Brisbane: Australian Coal Association Research Program (ACARP).

Enright, P. (1995). *Chronical of Awaba Colliery.* Newcastle, NSW.

Esterhuizen, G. S., Mark, C., & Murphy, M. M. (2010, July 27–29). *Numerical model calibration for simulating coal pillars, gob and overburden responses.* Paper presented at the 29th international conference ground control in mining, Morgantown, WV.

Frith, R., & Creech, M. (1997). *Face width optimisation in both longwall and shortwall caving environments.* ACARP end of grant report C5015 (pp. 96). Brisbane: Australian Coal Association Research Program (ACARP).

Frith, R., Colwell, M., Shepherd, J., & Seedsman, R. (1992a). *Literature survey relating to longwalling at low depths of cover – Longwalls east of the freeway, Cooranbong Colliery.* ACIRL consulting report CGE/1327/3. Australian Coal Industry Research Laboratories.

Frith, R. C., Stewart, A. M., & Price, D. (1992b, July 7–10). *Australian longwall geomechanics – A recent study.* Paper presented at the 11th international conference ground control in mining, Wollongong.

Gale, W. J. (2004, August 3–5). *Rock fracture, caving and interaction of face supports under different geological environments. Experience from Australian coal mines.* Paper presented at the 23rd international conference ground control in mining, Morgantown, WV.

Gale, W. J. (2009). *Matching longwall support design to industry requirements in weak ground.* ACARP end of grant report C14030 (pp. 55). Brisbane: Australian Coal Association Research Program (ACARP).

Galvin, J. M. (1981). *The mining of South African thick coal seams – Rock mechanics and mining considerations.* PhD thesis, University of the Witwatersrand, Johannesburg.

Galvin, J. M. (1982). *Total extraction of coal seams: The significance and behaviour of massive dolerite sills.* Research report no. 19/82 (pp. 80). Johannesburg: Chamber of Mines of South Africa Research Organisation.

Galvin, J. M. (1983, April 10–15). *The development of the theory of dolerite sill behaviour.* Paper presented at the 5th congress International Society Rock Mechanics, Melbourne.

Galvin, J. M., Steijn, J. J., & Wagner, H. (1981). Chapter 4: *Rock mechanics of total extraction.* Paper presented at the SAIMM vacation school on increased underground extraction of coal, Johannesburg.

Galvin, J. M., Steijn, J. J., & Wagner, H. (1982). Rock mechanics of total extraction. In C. J. Fauconnier & R. W. O. Kirsten (Eds.), *Increased underground extraction of coal* (pp. 69–110). Johannesburg: SAIMM.

Galvin, J. M., Hocking, G., & Anderson, I. (1994). *Pillar and roadway mechanics – Stage 1 – Introductory principles and practice,* Sydney: Key Centre for Mines – University of New South Wales.

Gupta, R. N., & Ghose, A. K. (1992, July 7–10). *Strata support interaction on a powered support longwall face under a massive dolerite sill – A study.* Paper presented at the 11th international conference ground control in mining, Wollongong.

Haramy, K. Y., & Fejes, A. J. (1992, July 7–10). *Characterization of overburden response to longwall mining in the western United States.* Paper presented at the 11th international conference ground control in mining, Wollongong, Australia.

Hardman, D. R. (1971). *Longwall mining under dolerite: Sigma Colliery Panel No. 4.* Research report no. 9/71

(pp. 38). Johannesburg: Chamber of Mines of South Africa Research Organisation.

Hatherly, P., & Luo, X. (1999, June 15–18). *Microseismic monitoring – Implications for longwall geomechanics and its role as an operational tool*. Paper presented at the 2nd international underground coal conference, Sydney.

Hatherly, P. J., Luo, X., Dixon, R., McKavanagh, B., Barry, M., Jecny, Z., & Bugden, C. (1995). *Roof and goaf monitoring for strata control in longwall mining*. ACARP end of grant report C3067 (pp. 76). Brisbane: Australian Coal Association Research Program (ACARP).

Henderson, P. G. (1980). Experience in longwall mining at Coalbrook Collieries. *The Journal of The South African Institute of Mining and Metallurgy, 80* (1), 22–33.

Holt, G. (1989). *Hydrofracturing trials to control massive roof at Newstan Colliery*. Paper presented at the longwalling in the 90s. ACIRL coal operators' conference, Sydney.

Jacobi, O. (1956, October 17–18). *The pressure on seam and goaf*. Paper presented at the international strata control congress, Essen.

Kelly, M., & Gale, W. (1999). *Ground behaviour about longwall faces and its effect on mining*. ACARP end of grant report C5017. Brisbane: Australian Coal Association Research Program (ACARP).

Kelly, M., Gale, W., Hatherly, P., Balusu, R., & Luo, X. (1996). *New understanding of longwall caving processes: Results of microseismic monitoring and initial computational modelling at Gordonstone Mine*. Paper presented at the symposium on geology in longwall mining, Sydney. Coalfield Geology Council of New South Wales.

Kelly, M., Gale, W., Luo, X., Hatherly, P., Balusu, R., & Smith, G. L. (1998, July 14–17). *Longwall caving process in different geological environments – Better understanding through combination of modern assessment methods*. Paper presented at the international conference geomechanics/ground control in mining and underground construction, Wollongong.

Kezdi, A. (1952). *Talajmechanika* [Soil mechanics]. Budapest: Tankonyvkiado.

King, H. J., & Whittaker, B. N. (1971). *A review of current knowledge on roadway behaviour*. Paper presented at the symposium on roadway strata control, London.

Latilla, J. W., & van Wijk, J. J. (2003, September 8–12). *Shortwall facebreak beneath a Dolerite Sill – Learning points from a recent event at Matla Coal Mine*. Paper presented at the 10th Congress International Society Rock Mechanics, Sandton, South Africa.

Laubscher, D. H. (1994). Cave mining – The state of the art. *The Journal of The South African Institute of Mining and Metallurgy, 94*(10), 279–293.

Mark, C. (1992). *Analysis of longwall pillar stability (ALPS): An update*. Paper presented at the workshop on coal pillar mechanics and design, Sante Fe, NM.

Mark, C., & Bieniawski, Z. T. (1987, June 9–11). *A new method for sizing longwall pillars based on field measurements*. Paper presented at the 6th international conference ground control in mining, Morgantown, WV.

Mark, C., Gauna, M., Cybulski, J., & Karabin, G. (2011, July 26–28). *Application of ARMPS (Version 6) to practical pillar design problems*. Paper presented at the 30th international conference ground control in mining, Morgantown, WV.

MDG-1017. (1994). *Roof support guidelines for massive strata conditions*. Sydney: NSW State Government.

Menzies, R. A. (c1970). *Roof support in coal mines*. Sydney: NSW State Government.

Mills, K. W., & O'Grady, P. (1998, February 18–20). *Impact of longwall width on overburden behaviour*. Paper presented at the Coal 1998: Coal operators' conference, Wollongong.

Moerdyk, C. M. (1965). *Historical and technical review of the Coalbrook disaster*. GME 16/20/12A. Johannesburg: Government Mining Engineer, South African Government.

Moodie, A., & Anderson, J. (2011, February 10–11). *Geotechnical considerations for longwall top coal caving at Austar Coal Mine*. Paper presented at the Coal 2011: Coal operators' conference, Wollongong.

MSEC. (2007). *General discussion on systematic and non systematic mine subsidence ground movements*. Retrieved from http://www.minesubsidence.com/index_files/files/General_Disc_Mine_Subs_Ground_Mvmnts.pdf

Nomikos, P. P., Sofianos, C. E., & Tsoutrelis, C. E. (2002). Structural response of vertically multi-jointed roof rock beams. *International Journal Rock Mechanics and Mining Sciences, 39*(1), 79–94.

Pappas, D. M., & Mark, C. (1993). *Behaviour of simulated gob material*. Report of investigation RI 9458 (pp. 45), U.S. Bureau of Mines.

Pells, P. J. N., & Best, R. J. (1991). Aspects of primary support design for tunnels in the Sydney Basin. *Transactions IEAustralian Civil Engineering, 33*(2), 57–66.

Peng, S. S. (2008). *Coal mine ground control*, West Virginia University.

Peng, S. S., & Chiang, H. S. (1984). *Longwall mining* (1st ed.). New York: Wiley.

Ryder, J. A., & Wagner, H. (1978). *2D analysis of backfill as means of reducing energy release rates at depth*. Research report no. 47/78. Chamber of Mines of South Africa Research Organisation.

Salamon, M. D. G. (1966). *Reconsolidation of caved areas*. Research report 38/66. Johannesburg: Transvaal and Orange Free State Chamber of Mines Research Organisation.

Salamon, M. D. G. (1974, September 1–7). *Rock mechanics of underground excavations*. Paper presented at the 3rd congress International Society Rock Mechanics, Denver, CO.

Salamon, M. D. G. (1983). *Rock mechanics: Its past, present and future*. Paper presented at the annual workshop of the Generic Mineral Technology Centre, Blacksburg, USA.

Salamon, M. D. G. (1990, 18–20 June). *Mechanism of caving in longwall coal mining*. Paper presented at the 31st US rock mechanism symposium, Denver, CO.

Salamon, M. D. G. (1991). Behaviour and design of coal pillars. *Coal Journal – Australian Journal Coal Mining Technology and Research, 32*, 11–22.

Salamon, M. D. G., & Oravecz, K. I. (1976). *Rock mechanics in coal mining* (Vol. P.R.D. series no. 198). Johannesburg: Chamber of Mines of South Africa.

Salamon, M. D. G., Oravecz, K. I., & Hardman, D. (1972). *Rock mechanics problems associated with longwall trials in South Africa*. Research report no. 6/72 (pp. 35). Chamber of Mines of South Africa Research Organisation.

Schumann, E. H. R. (1982). *Pillar extraction at Greenside Colliery*. Research report no. 15/82. Johannesburg: Chamber of Mines of South Africa Research Organisation.

Seedsman, R. W. (2004, 31 October – 2 November). *Back analysis of sub-critical subsidence events in the Newcastle Coalfield using voussoir beam concepts*. Paper presented at the 6th triennial conference. Mine Subsidence Technological Society, Maitland.

Singh, S. (2000). *Caving behaviour and related geotechnical issues associated with coal extraction beneath massive roof strata*. PhD thesis, University of New South Wales, Sydney.

Strawson, C., & Moodie, A. (2007, 31 July – 2 August). *Moranbah North tests the critical caving theories*. Paper presented at the 26th international conference ground control in mining, Morgantown, W.V.

Tulu, I. B., & Heasley, K. A. (2011, June 26–29). *Investigating the mechanics of pillar loading through the analysis of in-situ stress measurements*. Paper presented at the 45th US rock mechanics/geomechanics symposium, San Francisco, CA.

Vandergrift, T., & Conover, D. (2010, 26 July). *Assessment of gate road loading under deep Western U.S. conditions*. Paper presented at the 3rd international workshop on coal pillar mechanics and design, Morgantown, WV.

Wade, L. V., & Conroy, P. J. (1980). Rock mechanics study of a longwall panel. *Mining Engineering, 32* (12), 1728–1734.

Wagner, H. (1991). *Strata control principals of total extraction*. Paper presented at the design and extraction of underground coal reserves, Johannesburg.

Wagner, H. (1994). *Coal strata control handbook*. Unpublished.

Wang, Y., & Peng, S. S. (1996). *High horizontal stress effects on longwall gate entry stability*. Paper presented at the 15th international conference ground control in mining, Golden, Colorado.

Whittaker, B. N., & Reddish, D. J. (1989). *Subsidence. Occurrence, prediction and control*. Amsterdam: Elsevier.

Wilson, A. H. (1986, August). *The problems of strong roof beds and water bearing strata in the control of longwall faces*. Paper presented at the conference on ground movement and control related to coal mining, Wollongong.

Wold, M. B., & Pala, J. (1986, August). *The response of powered supports and pillars to initial longwalling under a strong main roof*. Paper presented at the conference on ground movement and control related to coal mining, Wollongong.